UNITED STATES
DEPARTMENT OF THE INTERIOR
GEOLOGICAL SURVEY

THE TRIASSIC CHITISTONE LIMESTONE,WRANGELL MOUNTAINS, ALASKA– STRESSING DETAILED DESCRIPTIONS OF SABKHA FACIES AND OTHER ROCKS IN LOWER PARTS OF THE CHITISTONE AND THEIR RELATIONS TO KENNECOTT-TYPE COPPER DEPOSITS

OPEN-FILE REPORT 77-217

This report is preliminary and has not been edited or reviewed for conformity with Geological Survey standards and nomenclature

Menlo Park, California
March 1977

Contents

Illustrations

The Triassic Chitistone Limestone, Wrangell Mountains, Alaska--stressing detailed descriptions of sabkha facies and other rocks in lower parts of the Chitistone and their relations to Kennecott-type copper deposits

by

Augustus K. Armstrong and E. M. MacKevett, Jr.

U.S. Geological Survey, Menlo Park, Calif.

ABSTRACT

Recent investigations show that sabkha deposits were important in the genesis of Kennecott-type copper ore. Massive chalcocite-rich lodes at Kennecott and nearby deposits formed in the lower 110 meters of the Upper Triassic Chitistone Limestone. The Chitistone and superimposed Upper Triassic and Jurassic sedimentary rocks formed in a marine basin on and surrounded by the Nikolai Greenstone, a thick, extensive, largely subaerial succession of tholeiitic basalt with intrinsically high copper content. Lowermost 110 meters of the Chitistone contains three incomplete upward-shoaling lime mud cyclic sequences that each consist of shallow subtidal limestone grading upward to intertidal stromatolitic fine-grained dolomite. The youngest cycle contains well-developed sabkha features and dolomitic pisolitic and laminate crust caliches and underlies shallow-marine limestone. The ore deposits are related to the youngest supratidal cycle. This carbonate cycle

represents a regional sabkha facies that developed between 90-110 meters above the Nikolai Greenstone. This facies, which contained abundant gypsum-anhydrite, was exposed to vadose weathering that leached much gypsum-anhydrite and developed a vuggy zone interbedded with porous dolomitic caliche zones. Subsequent marine deposition capped the porous zone with an impermeable seal.

The youngest sabkha horizon served as a permeable conduit for the ore-forming solution and was instrumental in localizing the major Kennecott-type ores.

INTRODUCTION

Purpose and scope

This paper focuses on detailed stratigraphic and petrographic studies of lower parts of the Triassic Chitistone Limestone, the hostrock for Kennecott-type copper deposits. It attempts to relate ore deposition to the influence of stratigraphic and sedimentary controls within the carbonate section and, additionally, provides detailed information on the carbonate petrography, stratigraphy, and related topics of the well-exposed lower Chitistone stratigraphic outcrops (figs. 1, 2, and 3). The present report elaborates on an earlier report (Armstrong et al., 1969) and refines the previous work by concentrating on detailed studies of lower parts of the Chitistone and by discussing additional localities.

Study area

The study area is along the southern flank of the Wrangell Mountains (fig. 1) where the Chitistone Limestone is best developed and hosts the major Kennecott-type copper deposits. This paper is largely based on detailed studies of rocks from 5 stratigraphic sections of lower parts of the Chitistone that were measured in 1974. The report is supplemented by data derived from previously studied stratigraphic sections (Armstrong et al., 1969; Armstrong and MacKevett, 1976; fig. 1) and, to some extent, by broad-scope geologic studies of the McCarthy quadrangle that are summarized in MacKevett (1976).

Work Methods

Field studies conducted in 1974 focused on detailed stratigraphic studies of the lower 140 m of the Chitistone Limestone with particular attention given to sedimentary structures and sampling. Oriented thin sections of numerous specimens representative of the outcrop sections and underground exposures were studied petrographically. Friedman's (1959) methods were used for staining thin sections. Alizarin red was used for calcite and potassium ferricyanide was used for ferrous iron in dolomite. Polished rock specimens were etched for 60 seconds in 1 molar HCl for study under the Scanning Electron Microscope (SEM).

The methods used for pre-1974 studies that are integrated into this report are discussed in Armstrong, MacKevett, and Silberling (1969). They are similar to those of the present study except they lack SEM data.

The carbonate rock classification used in this report is from Dunham (1962).

GEOLOGIC SETTING

The distribution and structural relations of the Chitistone Limestone are discussed in several reports relevant to the McCarthy quadrangle, notably MacKevett (1965, 1970, 1974, 1976). The Chitistone occupies a northwest-trending belt along the southern flank of the Wrangell Mountains, almost entirely in the McCarthy 1 by 3 degree quadrangle. Chitistone outcrops are known at a few Alaskan localities north of the Wrangell Mountains and in the Yukon Territory (MacKevett, 1976). The Chitistone disconformably overlies a thick platform of Nikolai Greenstone [late Middle and(or) early Late Triassic], which consists of tholeiitic basalt that for the most part was extruded under subaerial conditions. Recent paleomagnetic investigations indicate that the Nikolai Greenstone formed at low paleolatitudes in the proto-Pacific Ocean (Hillhouse, 1977, in press). Inasmuch as the Nikolai and Chitistone are components of the same cohesive tectonic terrane, it is implicit that the Chitistone formed in a similar paleoenvironment. The lowermost 130 m of the Chitistone contains carbonate rocks that formed in supratidal and intertidal depositional environments. This sequence is superseded by limestone of shallow marine origin, which dominates stratigraphically higher parts of the Chitistone. The Chitistone grades upward into more open marine carbonates of the Nizina Limestone, of Late Triassic age, which, in turn, grade upward into the McCarthy Formation, of Late Triassic and Early Jurassic age. This gradation reflects a general progressive deepening of the marine depositional environments. Deformation and local metamorphism of the Chitistone are mainly consequences of a regional orogeny during parts of the Late Jurassic and Early Cretaceous.

DESCRIPTIONS OF MEASURED STRATIGRAPHIC SECTIONS[1/]

[1/] In this report all stratigraphic positions are given in meters above the Nikolai Greenstone-Chitistone Limestone contact; 85 m means 85 m above the base.

The Chitistone Limestone outcrops at Donoho Peak (74A-4T), Green Butte (74A-3T), and Nizina River (74A-7T) are in stratigraphic order and unaffected by faulting or metamorphism throughout their lowermost 140 m (figs. 4, 5). The Erie mine section was measured to a horizon some 105 m above its base where dolomitization and tectonic fracturing have obscured stratigraphic relationships.

A smooth flat surface marks the top of the Nikolai Greenstone, but evidence of extensive pre-Chitistone subaerial weathering of the Nikolai is lacking. This lack of weathering may be due in part to wave cutting by the initial marine Chitistone transgression over the Nikolai Greenstone and removal of the ancient regolith.

The basal Chitistone consists of gray-yellow calcareous shale and nodular argillaceous lime mudstone, 0.3-2 m thick, in sharp contact with the underlying Nikolai Greenstone. The Chitistone Limestone from 2 to 10 m is massive, gray, and composed of lime mudstone that contains fragments of mollusk shells preserved as micritic envelopes with sparry calcite fillings. The lime mudstone beds are typically composed of calcite crystals between 2 to 6 um in size and argillaceous material; above 10 m they consist of calcite rhombs in the 10 to 50 um size range (fig. 6, A).

At the Donoho Peak section, a thin-bedded platy argillaceous, dark-gray pelletoid lime mudstone to packstone occurs between 24 to 26 m. It is overlain by a 1-m-thick pellet to mud-lump lime mudstone and packstone. A 1-m-thick bed of slightly argillaceous, dark-gray dolomitic lime mudstone at 30-31 m contains laminae that are interpreted as weakly developed algal mat structures. Park (1976, fig. 1a) and Kinsman and Park (1976) state lamination is an intrinsic characteristic of stromatolites, and Park's figure 1a shows sedimentary features similar to those from the 30-31 and 47-48 levels. This laminated mudstone is composed of pellets with some micrite (fig. 6, B). The laminations in part reflect alternating bands of different dolomite contents. The Donoho Peak limestones from the 31- to 47-m interval are similar to the underlying beds except for a well-developed (38 to 43 m) of dark-gray argillaceous, platy pelletoid dolomitic lime mudstone and packstone.

A pelletoidal packstone from 37 m (fig. 6, C) is typical of the nonargillaceous carbonate rocks of this interval. Similar pelletoidal packstones are found to 55 m in the Nizina River section. These pellets commonly contain subhedral dolomite rhombs and local micritic envelopes, and they are coated with fibrous calcite (fig. 7, B, C). Spaces between the pellets are filled by microspar or sparry calcite cement.

At the Donoho Peak section a stratigraphic level between 47 to 48 m is laminated dark-gray argillaceous dolomitic lime mudstone (fig. 6, D) lithologically similar to the bed at 31 m. The higher bed contains thinner, better developed laminae. Alizarin red staining of thin sections reveals alternating bands of dolomite-rich and dolomite-poor carbonate minerals. The section from 49 to 93 m at Donoho Peak and 59 to 85 m at the Nizina River section (fig. 7, D) contains some dolomite rhombs but is primarily pelletoid-molluscan-echinoderm lime mudstones and wackestones. The SEM photomicrograph of a specimen from Donoho Peak at 69 m (fig. 6, E) shows the pellets are composed of 2- to 6-um-size calcite rhombs and micrite between pellets of calcite rhombs in the 8- to 20-um size and some subhedral dolomite in the 10- to 15-um size range. The limestone from 72 m at Donoho Peak is typical pelecypod-gastropod-echinoderm, pelletoid dolomitic wackestone to packstone. Above 86 m bioclasts of mollusks and other invertebrates are rare or absent. SEM photomicrographs (fig. 6, F) of peloid packstone at 88 m shows the pellets again are composed of smaller size calcite rhombs, 5 um long, but contain more clay between rhombs than the adjacent micrite matrix, which has calcite rhombs 5 to 20 um in size. A similar sequence is found in the Nizina River section from 59 to 85 m (fig. 7, B, C) and are composed of lime mudstone and peloid packstone with 10 to 35 percent dolomite that forms euhedral to subhedral rhombs 10-60 um in size. The lack of fossil remains and abundance of peloids both indicate a restricted, probably subtidal to intertidal, depositional environment for the dolomitic limestone. The Green Butte section from 24.5 to 87 m shows similar lithologies (fig. 8, D-F). At Donoho Peak at 94 to 98 m and at 86 to 122 m at the Nizina River sections the rocks are brownish-gray dolomite with calcite void fillings. Some beds contain well-preserved pelletoid texture and relict fragments of echinoderms.

The composition of microfacies from 97 to 105 m at Donoho Peak is complex (fig. 9), but the rocks are predominately dolomitic. The stratigraphic interval between 97 to 99.5 m is composed of brownish-gray dolomite with abundant 2- to 15-cm-size vugs filled with dolomite and calcite. At about 97-100 m is a 25- to 40-cm-thick bed of dolomitic limestone (fig. 10, A, B, E; fig. 11) consisting of dolomitic mudstone, peloids, and laminated crust. The vugs or cavities in these beds are lined with large, up to 0.5- to 1-mm-size, rhombs of limpid dolomites with superposed sparry calcite. A 5- to 10-cm-thick bed of yellowish-orange, pyritic, argillaceous dolomite is interbedded within this unit.

Intertidal-supratidal sedimentary features are found in the Nizina River section at 86, 90, and 94-96 m (fig. 7, E-F). The algal mats at 94 m are associated with laminated crust and pisooids. The sedimentary structures at 95 m contain vugs filled by dolomite and calcite. These cavities are lined with large, 1-2 mm, subhedral to euhedral limpid dolomite rhombs and are partly filled with sparry calcite. The beds exposed at the 95-m level have the characteristic gray dolomitic matrix and white dolomite and calcite vug fillings that are lithologically similar to the zebra beds associated with the ore bodies in the Mother Lode, Bonanza, and Jumbo mines (fig. 4). Massive dolomite that is chert free and contains no obvious sedimentary structures occurs between 97 and 122 m. Some beds may be composed of dolomite rhombs as large as 1 mm. The brown dolomites from 122 to 135 m contain black nodular chert. The sedimentary structures at 129 and 135 m (fig. 8, A-C) are well-developed dolomitic-limestone peloids. Dolomite and calcite void fillings are found at 131 m above the base. An intriguing sedimentary structure, a sedimentary breccia, occurs at 130 m (fig. 12, A, D). Voids between the dolomite clasts of the breccia apparently were initially filled by radiaxial fibrous dolomite and subsequently by radiaxial calcite superseded by blocky calcite.

The Green Butte section has yellowish-brown-gray dolomite (90 to 101 m), and dolomite with dolomitic pisooids and laminated crust (fig. 8, D-F) in its upper part (101 to 103.5 m). At 103.5 m are massive, gray, algae-molluscan-echinoderm wackestones and packstones that are interpreted as representing a regional marine transgression.

At Donoho Peak at about 101 to 104 m is calcitic dolomite which has the relict texture of a molluscan-ostracode wackestone-packstone. The fossil fragments were molds that are now filled by dolomite in the 50- to 100-um-size rhombs.

The section at Donoho Peak from 104 to 122 m shows evidence of a marine transgression, by a decrease in dolomite, and an increase of limestone with abundant remains of mollusks, echinoderms, and brachiopods (fig. 7, A).

Chitistone Limestone section 74A-2T on Bonanza Ridge was measured about 600 m south of the Bonanza mine (fig. 13). The Chitistone near the main Kennecott mines from west of the Jumbo mine to McCarthy Creek has been extensively dolomitized, brecciated, and faulted. Outcrops on Bonanza Ridge are difficult to correlate with nearby outcrop sections at Donoho Peak to the west (74A-4T), or at Green Butte mine to the southeast (74A-3T) (fig. 4). However, limestones in the stratigraphic interval 4 to 18 m above the Nikolai provide reasonably valid stratigraphic correlations. These basal beds are 1 to 2 m of calcareous shales and thin-bedded argillaceous lime mudstones and 9 to 10 m of bioturbated, argillaceous, gray, thin-bedded lime mudstone. Characteristic structure of these beds are "crinkly" bedding surfaces formed by anastomosing tracks, trails, and burrows. The lime mudstone is composed of 5- to 15-um-size crystals of calcite (fig. 14, A). The Chitistone Limestone at about 20 m above the Nikolai has been brecciated and altered to medium- and coarse-grained dolomite.

The Chitistone Limestone on Bonanza Ridge from west of the Jumbo mine east to McCarthy Creek and in section 74A-2T is extensively dolomitized except for the lower 20-30 m of the section (figs. 4, 13). Outcrop and petrographic studies suggest the following sequence of events.

(1) Deposition of the Chitistone Limestone on the Nikolai Greenstone. Development of a few thin beds of early diagenetic dolomite. The original stratigraphic sequence probably was similar to the relatively unaltered sections at Donoho Peak, 74A-4T, and Nizina River, 74A-5T.

(2) A late stage, possibly low temperature hydrothermal dolomitization of the entire Chitistone Limestone on Bonanza Ridge, except for the lower 20-30 m. These lower beds may have remained undolomitized due to the higher argillaceous content and possible lower porosity and permeability to the magnesium-bearing fluids.

(3) Tectonic fracturing, which resulted in the formation of numerous 10-um- to 0.5-mm-wide fractures and in some beds the formation of angular dolomite breccias.

(4) The circulation through the rocks of magnesium-rich fluids, which deposited or lined the larger cavities with 0.4- to 4-mm-zoned dolomite rhombs. There is no clear-cut evidence in the thin sections that the large dolomite rhombs which line the cavities were not the final stage of dolomitization of the original limestone.

(5) The introduction of calcium carbonate-rich fluids that deposited sparry calcite in the fractures and remaining voids of the breccias and intercrystal spaces in the dolomites. This phase may be responsible for much of the dedolomitization (calcification) in some of the dolomites and the large dolomite rhombs that line the vuggy and brecciated beds.

The Bonanza Ridge outcrops are so altered by the coarse dolomitization and so brecciated that many of the regional marker beds of the Chitistone Limestone were obliterated. These include the first and second laminated beds which are well developed at Donoho Peak section 74A-4T and Erie mine section 74A-6T. We found in 1977 the outcrops of the zebra beds in the middle part of the Glory Hole diggings, above the old power plant of the Bonanza mine. The zebra beds are poorly exposed in outcrops near the Kennecott mines because of local faulting and brecciation, but they are well developed and exposed underground in the Mother Lode, Bonanza, and Jumbo mines.

The extensive, coarse-grained dolomite associated with ore are believed to reflect a late stage, probably low-temperature, hydrothermal episode. The reasons for this interpretation are:

(1) Dolomitization cuts across the stratigraphic section, irrespective of the original fabric or environments of depositions.

(2) The dolomite is fairly coarse with dolomite rhombs generally 100 um or larger in size.

(3) Stratigraphic sections at Donoho Peak 74A-4T and at the Nizina River 74A-7T contain dolomite zones restricted to horizons with subtidal to supratidal sedimentary structures that probably resulted from early diagenetic processes.

INTRAFORMATIONAL STRATIGRAPHIC CORRELATION AND ENVIRONMENTS OF DEPOSITION

The correlations shown in figure 4 for the lower part of the Chitistone Limestone are based on sedimentary features and microfacies. The interpretation of carbonate microfacies, sedimentary structure, and depositional models (fig. 15) follow the stratigraphic concepts published by Wilson (1970, 1975).

The lower 100 to 120 m of the Chitistone Limestone exposed from Donoho Peak to the Nizina River outcrops fits in Wilson's (1975, p. 297) classification of upward-shoaling carbonate sediment cycles that are composed predominately of lime mudstone (micritic) sediments whose faunas and sedimentary structures show a progressive upward change through restricted shallow marine carbonates with megafossils to dolomites and caliches. In these cycles a sharp upper contact occurs with open marine beds at the base of the next cycle. Work on the modern sabkhas has shown that the saline supratidal flats are aggradational features which gradually extend over subtidal, intertidal, and lagoonal sediments (Evans et al., 1964; Purser and Evans, 1973). Wood and Wolfe (1969) described in detail 9 similar sabkha cycles from the Late Jurassic and Early Cretaceous Arab/Darb Formation of Arabia. Similar cycles were described by Wilson (1967) from the Duperow Formation (Devonian) of the Williston basin, western North Dakota and adjacent areas. The Duperow contains 12 such cycles. Wilson estimated the time of each cycle is about 500,000 to a million years.

The well-exposed Donoho Peak section, 75A-4T (fig. 16), is the best outcrop for interpreting environments of deposition for the lower 130 m of the Chitistone Limestone (figs. 4, 16).

The Chitistone Limestone as shown on figure 4 contains two well-developed physical correlation lines. One is the contact with the Nikolai Greenstone.

The second, which is exposed in three of the measured outcrop sections, is the dolomitic-peloid-pisoolitic laminated caliche beds that range from 30 cm to greater than 1 m in thickness. The caliche horizons are developed at the Nizina River section 74A-7T at 135 m, the Green Butte section 74A-3T at 101-102 m and at the Donoho Peak section 74A-4T at 97 to 98 and 99.8 to 100 m. Our underground studies in 1977 found a 60-cm-thick bed of dolomitic-pisoolitic laminated caliche above the zebra beds in the 503-m (1650-ft) level of the Mother Lode mine.

The lower half of the Chitistone Limestone can be correlated between the Donoho Peak section 74A-4T and the Erie mine section 74A-6T by two weakly developed incomplete upward-shoaling lime mud (micrite) cycles that are developed at the 30- to 35-m and 48- to 52-m levels. These lower incomplete carbonate deposition cycles were not recognized in the Bonanza mine outcrop section, 74A-2T (probably due to faulting), or at the Green Butte section 74A-3T.

The incomplete carbonate deposition cycles that occur at 48 to 52 m at the Donoho Peak and Erie mine sections are probably a time-stratigraphic equivalent to the laminate-pisoid caliche bed found between 86 to 96 m in the Nizina River section 74A-7T.

The underground Mother Lode mine section shown on figure 4 is about 5 m thick. Similar lithologies are found in the Jumbo and Bonanza mines near bases of the ore bodies. This lithology, referred to as the zebra beds, is associated with intertidal to supratidal sedimentary structures and from drill hole data is known to be about 103 m above the Nikolai Greenstone (P. R. Holdsworth, oral commun., 1974). The ore bodies at the Mother Lode mine are stratigraphically higher than the other known Kennecott ore bodies, Jumbo and Bonanza Mines. It contains similar sedimentary features found at 96 to 104 m at the Donoho Peak section, 101 to 104 m at the Green Butte section and 95 m and also at 129 to 135 m at the Nizina River section. The dolomite and sedimentary structures at 129-135 m at the Nizina River section is correlated, as shown on figure 4, with the other sections, because it is the final supratidal cycle in this outcrop, contains the best sabkha features and the best developed caliche zone, and is overlain by pelecypod-echinoderm, packstone that represents the second major regional marine transgression above the Nikolai Greenstone.

AGE OF THE CHITISTONE LIMESTONE

Age diagnostic fossils are rare in the Chitistone Limestone. The Chitistone's age, Karnian Stage of the Late Triassic, is best documented by ammonites of the genus *Tropites*, which are widely, but sparsely, distributed in the stratigraphically medial and upper parts of the formation.

Silberling (*in* Armstrong, MacKevett, and Silberling, 1969) stated, "A fauna comprising *Tropites* cf. *T. welleri* Smith, *Arcestes*, and *Halobia* cf. *H. superba* Mojsisovics, was collected about 152 m above the base of the Chitistone at Green Butte (USGS Mesozoic loc. M1707) and is indicative of a late Karnian age."

DISCUSSION OF SPECIFIC SEDIMENTARY FEATURES

Lime mudstone and micritic matrix

The lower 100-120 m of the Chitistone Limestone fits Shinn et al.'s (1969) description of subtidal to supratidal carbonate sedimentation and is an example of Wilson's (1975) upward-shoaling lime mud (micrite)-sabkha cycles. The micrite facies is the dominant rock type in facies belts 8 and 9 (fig. 15). Matrix is intergranular material and it is usually composed of carbonate mud. Bathurst (1971, p. 511) stated the upper limits of lithified micrites is 3-4 um. The SEM photomicrographs of micrite crystals from the Chitistone Limestone from the Donoho Peak section, 74A-4T, shows micrite crystals somewhat larger in size. At 4 m they range from 5 to 15 um; at 37 m they are between 3 and 7 um (fig. 6, C); and at 88 m they are from 4 to 15 um (fig. 6, F). The Nizina River section, 74A-7T, shows similar large crystals in the lime mudstone. There the lime mudstone at 10 m has micrite crystals from 5 to 20 um and at 42 m from 5 to 30 um (fig. 10, B, C). Dolomitic limestones at 74 m show micrite crystals from 5 to 10 um (fig. 7, D).

Petrographic microscope and SEM studies of the Chitistone lime mudstones and micritic matrix shows the typical micrite crystals are generally in excess of 2 um in size and have been affected by aggrading neomorphism. The fuzzy outline of many of the peloids and some bioclastic material is the result of calcite neomorphism. In a strict sense many of the Chitistone lime mudstones could be classified as microspars (Folk, 1965).

Pellets

McKee and Gutschick (1969) applied the term peloid to allochems formed of cryptocrystalline or microcrystalline material irrespective of size or origin. This form would include lime mud (micrite) particles without laminae from 0.020 to 4 mm in size as shown on figure 4. Pellets or peloids can be formed as fecal pellets from any number of organisms, or by the process of micritization.

The lower part of the Chitistone Limestone contains abundant pellets and peloids. They may have well-defined shapes or blurred outlines (fig. 6, C).

Peloids with well-defined outlines (fig. 6, C; fig. 7, A) when examined by the petrographic microscope show a diagenetic sequence of events. These events are (fig. 17), the deposition of the peloids, a first stage $CaCO_3$ cement, filling of voids between peloids by sparry calcite cement and development within many of the peloids of euhedral rhombs of dolomite.

SEM examination of the peloids reveals in detail their crystal structure, inclusions of clay, and outlines. A specimen at 69 m from the Donoho Peak section shows (fig. 6, E) the peloid to be composed of calcite crystals in the 3-4 um size range, whereas the interpeloid cement is in the 7-20 um size range. A SEM photograph of a peloid packstone from 88 m (fig. 6, F) shows the peloids to be 100-300 um in diameter, formed by 2-3 um calcite rhombs, with abundant clay minerals between the calcite rhombs. The matrix between the peloids is very low in clay minerals and is formed by 5- to 20-um calcite rhombs.

Bioclast debris

Bioclastic debris is relatively rare within the lower part of the Chitistone Limestone and consists primarily of ostracode, pelecypod, gastropod, and echinoderm remains. Most of the pelecypods and gastropods were aragonite, and are now preserved as micritic envelopes. These fragments do not show the details of the original shells, but their original outlines are preserved as a dark thin outer zone that encloses an infilling of sparry calcite cement. Bathurst (1971, p. 333) considered these dark outer rims to be the results of the infilling of algal borings by carbonate mud, resulting in a micritic envelope. Logan et al. (1970, p. 62), in the Pleistocene Carbla Oolite of Shark Bay, Western Australia, found aragonitic fossils were dissolved preferentially, leaving moldic porosity, whereas calcitic skeletal material remains intact. The molds and intact fossils are set in a matrix of calcitic skeletal debris which is cemented by sparry calcite.

Sedimentary breccias

The Nizina River section contains a sedimentary breccia at the 130-m level above the Nikolai Greenstone (fig. 12, A-D). The breccia clasts may be up to 10 cm long and 3 cm thick and contain birdseye structure. Interclast cavities are elongated subparallel to bedding. The matrix of the clasts is composed of 100- to 150-um subhedral dolomite rhombs commonly separated by black, partly oxidized, pyrite cubes, 4 to 12 um in size. Surfaces of the clasts are lined with white elongate dolomite rhombs which extend 2 to 5 mm into interclast cavities (fig. 12, A-D). The coarse-grained dolomite is in turn overlain by gray radial axial calcite which extends 2 to 6 mm into the cavities. The remaining voids were partly filled by sparry calcite. Between the elongate dolomite rhombs and the radial axial calcite is a diffused band of disjunct 100- to 300-um quartz with calcite inclusions and associated scattered 20- to 30-um-size pyrite crystals.

The origin of the breccia is not clear. It is associated with beds that contain algal mats, peloids, and laminated crusts, features indicative of an intertidal to supratidal environment of deposition. All of the breccia clasts show fractures and fissures which indicate that the clasts must have been coherent and partially cemented. The fractures cut across the burrows and laminations of the clasts.

The sequence of events for the formation of these breccias appears to be (1) deposition as carbonate sediments in a subtidal-intertidal to possible supratidal environment; (2) partial cementation of the carbonate muds; (3) fracturing of the rigid sediments; (4) the matrix of the sediments may have originally been dolomite or was progressively changed from calcium carbonate to dolomite in the above stages. Coarse dolomite rhombs were deposited on cavity walls of the fractured and porous sediments. (5) The deposition of the radial axial fibrous calcite over the dolomite, which may represent recrystallized fibrous aragonite cement (Kendall and Tucker, 1973); (6) final void filling by coarse sparry calcite, which probably occurred in a fresh-water diagenetic environment. Eugene Shinn (written commun., 1976) interpreted the cements to be submarine (subtidal) in origin.

Origin

The stratigraphic association of the breccia with subtidal and supratidal sediments, sedimentary features such as clasts and burrows, and the lack of fossils all suggest these breccias were formed in a subtidal to intertidal environment. Evamy's (1973) study of the intertidal-supratidal sediments of the Trucial Coast of the Persian Gulf showed sedimentary structures similar to the Chitistone breccias. He described and illustrated intertidal cementation, brecciation and teepee structures which may be analogous to the Chitistone breccia. Robert Park (written commun., 1977) stated "Interclast conglomerates some of which have a breccia-like appearance are common in intertidal areas of Abu Dhabi. They occur either as lag deposits in very shallow (< 1/2 m) upper intertidal channels or on the lithified crests of slight highs in the intertidal areas, where it is commonly associated with crab activity."

Shinn (1969) described shallow, subtidal marine cementation and development of teepee structures from the Persian Gulf. These are associated with sediments which contain abundant molluscan and other shell fragments.

The sequence of carbonate minerals which fill the voids and cavities provides clues regarding the history and genesis of the Nizina breccia. The initial lining of the cavities by coarse dolomite rhombs indicates hypersaline brines and marine environments. Kendall and Tucker (1973) suggested radiaxial fibrous calcite, similar to that found in our breccias, is a replacement after acicular aragonite or fibrous magnesium calcite. Folk (1974) indicated that acicular carbonates are the result of slow sideward crystal growth in marine or tidal environments rich in magnesium. If these two assumptions are correct then the radial axial calcite was originally formed probably by marine waters.

Zebra beds and vug fillings

Examination of the underground workings of the Bonanza and Mother Lode mines shows a close spatial association between ore bodies and specific stratigraphic levels. The ore is commonly associated with the zebra beds, of the miners, that have specific carbonate rock fabrics, sedimentary structures, and environments of deposition. Zebra bed lithology is also known from the Nizina River section where it is found some 95 m above the Nikolai Greenstone (fig. 19, C).

The ore bodies in the Chitistone Limestone are generally 100-120 m above the Nikolai Greenstone contact, typically associated with the so-called "zebra beds." A photograph (fig. 18) and samples of these beds at the 503-m (1,650-foot) level, adjacent to a large ore body in the Mother Lode mine shows zebra beds that comprise a matrix of subhedral 50- to 200-um light-brown-gray dolomite with abundant flat-bottomed, cumulus, enterolithic-shaped vugs, now lined with light-gray to white zoned coarse dolomite. Centers of the vugs are partly filled with sparry calcite (fig. 14, B-F; fig. 19; fig. 20, B, D-F). Abundant 5- to 100-um-wide fractures cut the dolomite matrix, and both the dolomite and calcite vug fillings. These fractures are filled with sparry calcite and copper minerals. The intercrystalline pores between dolomite rhombs of the matrix contain sparry calcite. The outcrop specimen from the Nizina River section 74A-7, from 95 m above the Nikolai Greenstone (fig. 7, E, F), shows the same mineralogy and sequence of mineral events, except the fine fractures are filled with calcite and are devoid of copper minerals.

Fine-grained uniform dolomite that contains burrow and small-scale cut and fill structures underlies the zebra beds. The overlying beds are 1- to 3-m-thick beds of pisolitic-laminated crust caliche, followed by coarse-grained dolomites with dolomite pseudomorphs of crinoid bioclasts.

The zebra beds of the Mother Lode mine and the Nizina River section 74A-7 (fig. 18; fig. 14, B-F; fig. 19, A-E; fig. 20, B-F) show sedimentary structures similar to Stromatactis. Stromatactis was first used taxonomically by Dupont (1881) for distinctive crystalline carbonate features that he considered stromatoporoids in Devonian limestones of Belgium. Lecompte (1937, 1954) thought these features were precipitated calcite resulting from the decomposition of algae. Bathurst (1959) concluded *Stromatactis* refers only to an enigmatic flat-bottom crystalline feature.

The Chitistone Limestone zebra structures are parallel with the underlying and overlying beds. This relationship is well displayed in the inclined shafts of the Mother Lode and Bonanza mines. The shafts parallel the beds just below the zebra bed. At various levels from the inclined shaft there are drifts into or across the zebra beds. Observations within the mine suggest there are no mounds or topographic highs within the bedding. The parallel stratification of the zebra beds is well displayed by the outcrops west of the Bonanza mine on Bonanza Ridge and on the Nizina River (fig. 3). There is no indication in these or other outcrops examined of mounds or banks developed within the lower 150 meters of the Chitistone Limestone.

Stromatactis sedimentary structures are associated with lime mud banks. The lime mud banks may have hundreds of meters of relief above the adjacent deeper water sediments (Lees, 1961, p. 103, fig. 2; Lees, 1964; Schwarzacher, 1961, p. 1483, figs. 2-4; Ross et al., 1975). Most of the *Stromatactis* described are on inclined prograding beds and these sedimentary structures have an original angle of inclination in respect to adjacent horizontal beds.

The zebra beds of the Chitistone Limestone are parallel to the bedding and to adjacent horizontal well-stratified carbonate beds. Mud mounds or paleotopographic highs have not been recognized with any of the Chitistone Limestone exposures. The zebra beds in the Mother Lode, Bonanza, and Jumbo mines parallel the underlying beds and overlying crinoidal beds. This feature is well displayed in the inclined shaft which parallels bedding and descends to the bottom depths of the mines.

We interpret the zebra beds as having been deposited in a sabkha environment. The dolomite- and calcite-filled vugs are interpreted as pseudomorphs after anhydrite.

Kinsman (1966, 1969), Kinsman and Park (1976), Shearman and Fuller (1969), Fuller and Porter (1969), Purser and Evans (1973), and Evans et al. (1969) gave detailed descriptions and documentation of the sedimentation, sedimentary sequence, early diagenesis, and sedimentary structures of sabkhas of the Persian Gulf. They showed that the infilling of lagoons along the Trucial Coast by Holocene carbonate sediments has produced a supratidal coastal plain which extends along 241 km of coastline, is more than 16 km wide, and covers an area in excess of 2,590 square kilometers. High temperatures and low rainfall give rise to high net evaporation, which results in the formation of concentrated, sea-water-derived, interstitial brines. Interstitial precipitation of new minerals takes place, and reaction occurs between brines and initial aragonite sediments. Widespread dolomitization occurs. Gypsum is widely precipitated, mainly in the upper intertidal zone and seaward part of the coastal plain. Abundant anhydrite is precipitated interstitially in mid and inner parts of the coastal plain, above the water table. The anhydrite is nodular in form.

Kendall and Skipwith's (1969, p. 859) photographs of the trenches they dug in Holocene sabkha deposits of Abu Dhabi show nodular and contorted anhydrite that is parallel to the surface or bedding and which has nearly identical physical outlines and shapes as the strataform vugs shown on the tunnel wall in figures 18, 21, 19, and 20, B, D-F, from the Mother Lode mine, and from the Nizina River outcrop section 74A-7T at 95 m above the Nikolai Greenstone (fig. 20, C).

Evidence for a sabkha deposition environment for the zebra beds includes: (1) They are the top suite of beds of a sequence which goes from molluscan-peloid wackestones (subtidal) to beds dominately composed of dolomites and devoid of fossil fragments; (2) sedimentary structures and shapes of the dolomite- and calcite-filled vugs, their flat bottoms, and lenticular, enterolithic shape; (3) finer grained subhedral dolomite matrix; (4) the parallel conformity of the zebra structures and their beds with the overlying and underlying carbonate strata.

A suggested sequence of events for the formation of the zebra beds, as indicated from the study of the polished slabs, SEM and EDAX examination, and thin sections, is believed to be (fig. 21):

(1) The development of a coastal sabkha carbonate offlap facies in the Chitistone Limestone at a stratigraphic level of some 90-120 m above the Nikolai Greenstone. Framework sediment of the sabkha sediments was probably calcium carbonate, although no definitive evidence is preserved.

(2) Sabkha diagenesis of these carbonate sediments probably included dolomitization and concurrent emplacement of diagenetic gypsum and anhydrite nodules within the sabkha sediments (Kinsman, 1966, 1969).

(3) The dissolution of the gypsum and anhydrite nodules from the zebra beds with associated dedolomitization of some of the dolomite matrix. Field and petrographic studies do not clearly define the time in which this event occurs. The outcrop sections, at Donoho Peak 74A-4T, Green Butte 74A-3T, Nizina River 74A-6T, and the underground exposures in the Mother Lode mine have sequences that are interpreted as sabkha deposits containing beds that have dolomitic pisooid-laminated caliches. The caliche may represent regional developments of supratidal hypersaline brine vadose weathering (Scholle and Kinsman, 1974). During periods of vadose weathering, meteoric ground water may have penetrated and dissolved the gypsum or anhydrite nodules within the underlying sabkha sediments and formed the vugs.

(4) Deposition of coarse-grained, white, zoned dolomite on the walls of the vug. Petrographic evidence does not define the time of this event. The Nizina River outcrop beds and the samples from the zebra beds in the mines contain voids that are filled by limpid dolomite rhombs and sparry calcite. The void fillings and mineralogy of outcrop samples and mine samples are identical. The outcrop example suggests an early diagenetic origin for the large clear dolomite crystals. The extensive voids created by the removal of the gypsum-anhydrite (figs. 18, 21, 14, B-F; 19, 20) would indicate that a thick section of sediments above this zone would result in the collapse of the dolomite matrix framework and brecciation of the zebra zones. Thus it can be argued that the partial infilling of the vugs by coarse dolomite occurred at shallow depths and possibly in the sabkha environment. Folk and Land (1975, p. 63) gave theoretical arguments that dolomite probably forms most readily by a reduction in salinity, particularly in a schizohaline environment (alternating between hypersaline and near-fresh conditions) as in a floodable sabkha or a phreatic mixing zone. Flushing marine saline waters with fresh water lowers salinity but maintains a high Mg/Ca ratio; crystallization is slower and the interfering effect of foreign ions is reduced. They stated (p. 67) that dolomite formed from dilute solutions is characteristically limpid.

Folk and Siedlecka (1974) described limpid dolomites from late Paleozoic rocks of Bear Island, south of Spitsbergen. Their upper Carboniferous Fusulina limestone formation consists mainly of very finely crystalline subhedral dolomites. They believed it represented a hypersaline, sabkha-type deposition environment. Fractures and birdseye vugs in this fine dolomite are filled with coarse, sparry calcite and 50- to 100-um crystals of limpid dolomite. The calcite is younger and is a product of phreatic fresh-water diagenesis.

Folk et al. (1973) described limpid dolomite lining cavities that were later filled with poikilotopic sparry calcite from the Tertiary Bluff Limestone on Cayman Island, British West Indies.

(5) The event that formed the fractures that are 10 um to 0.5 m wide is clearly post-limpid dolomite formation. The fracturing may have occurred during or after the deposition of the coarse-grained sparry calcite that fills the remaining pore space in the vugs. Sparry calcite fills the fractures within the matrix and the intercrystalline porosity of the dolomite matrix. Deposition of this calcite was the last major event. If one accepts Folk and Land's (1975, p. 60) concept that blocky calcite can be formed only in low Mg/Ca water, that is derived from meteoric water or where Mg has been removed from marine water by formation of dolomite or absorption clays, it is possible the calcite is the product of phreatic fresh water. This is based on the purity of the calcite

and its large crystals. Fracturing and calcite void filling may have extended through several episodes as indicated by some calcite which fills voids and is then cut by fractures and filled by another cycle of calcite vein filling.

In the mines many of the fine fractures associated with the zebra beds contain not only sparry calcite but copper minerals. This occurrence indicates a late phase of copper mineralization in the long diagenetic history of these carbonate rocks.

Dedolomitization or calcification occurs in the rhombs of the fine-grained dolomite matrix and the limpid dolomite of the vugs adjacent to the sparry calcite and sparry calcite vein fillings of the zebra beds. Von Morlot (1848), Evamy (1963, 1967), and Shearman, Khouri, and Tara (1961) have shown that magnesium sulfate solution in the formation of dolomite, according to the equation: $2CaCO_3 + Mg^{++} + SO_4^{=} \rightleftharpoons CaMg(CO_3)_2 + CaSO_4$, and observed that this is a reversible reaction and suggested that gypsiferous solution could bring about dedolomitization. This dedolomitization can also be caused by meteoric water high in Ca^{2+}/Mg^{2+} ratios. Some thin sections show extensive calcification of dolomite rhombs adjacent to calcite-filled fractures.

Pellet, pisooid, and laminated caliche

Two lithologically distinctive and stratigraphically useful caliche marker beds are in the Donoho Peak section at 97 to 97.8 m and at 99.7 to 101 m. Similar caliche beds are at 102 m in the

Green Butte section, and at 135 m in the Nizina River section. The beds are from 0.3 to 1.3 m thick, weather a light-gray to light-yellowish-gray color and are easily recognized in the field by their color, the bands of laminated crust, and large peloid and pisooids up to 10 mm in diameter.

Thin sections and SEM studies show that the caliche is composed of dolomitic-micritic micropellets and large laminated pisooids in a micritic matrix with numerous voids filled by clear dolomite and sparry calcite. Nontectonic fractures are abundant (fig. 10, C; 11). The interparticulate voids and nontectonic fractures are filled first by clear limpid dolomite and then sparry calcite. The laminated crusts (fig. 10, B; fig. 7, F) are formed by undulating bands 10- to 100-um thick of dark-colored micrite separated by thin 10- to 500-um bands of light-colored to clear calcite and dolomite. The Chitistone Limestone laminated crust resembles closely the Quaternary laminated crust shown by Read (1974, p. 260, figs. 8a, b) from Shark Bay, Australia. Some dark-colored bands are separated by fibrous calcite up to 20 um in length (fig. 10, C); these may represent filled desiccation cracks.

The Chitistone caliches contain pisolites (fig. 11, A-C) and(or) large micritic peloids (fig. 7, B, C, F). The pisolites and peloids may be compound; those over 1 mm in size are usually irregular in shape. Reverse grading of pisolites is common (fig. 11, A, D). Fossil bioclasts are rare, and are generally small broken echinoderm fragments.

Scanning electron microscope photographs (fig. 8, A, B) of the pisooid caliche at 135 m in the Nizina River section clearly show the pisooids are composed of a mixture of 5- to 10-um-size calcite crystals and 0.5- to 10-um rhombs of dolomite. Large, 30- to 150-um, crystals of calcite and dolomite occupy spaces between the pisooids and are readily distinguished from carbonate crystals that form the pisooids. The bands of the pisooids are characterized by differing ratios or percentages of dolomite and calcite crystals (fig. 8, B).

The caliche zone at 100 m in the Donoho Peak section is characterized by well-developed laminated crusts (fig. 10, C, D).

The caliche zone at 102-103 m in the Green Butte section (fig. 8, E; fig. 20, A) contains well-developed peloids and laminated crusts. The pisolites are dolomitic and similar to those at the 135-m level in the Nizina River section.

The peloids, pisooids, and laminated caliche beds are all associated with carbonate sediments that indicate deposition in subtidal to supratidal environments. Esteban's (1976) classification would place these as vadose marine or vadose hypersaline caliche. Sedimentary structures in these beds are algal mats, dolomite and(or) interpreted calcite pseudomorphs after gypsum-anhydrite, and mud chips.

Examination by the SEM of the pellets and pisooids shows (fig. 8, A, C) they are dolomitic, generally with dolomite rhombs in the 0.5- to 10-um size range. Scholle and Kinsman (1974) and Purser and Loreau (1973) have shown that caliche crust on Pleistocene limestone in Abu Dhabi, Trucial Coast, Persian Gulf, and Bonaire, Netherland Antilles, form in supratidal vadose areas that are characterized, not by fresh water, but by hypersaline brines. The resultant textures of these crusts are largely vadose, but the mineralogy, aragonite and dolomite, and chemistry are of marine character. This environment could account for the abundance of microdolomite in the pisooids in Chitistone Limestone. It is suggested the Chitistone pisooids may have formed in part from dunes of skeletal grainstones, subjected to marine vadose weathering in hot semiarid conditions under the influence of fluctuating saline brines and rain water (schizohaline environment of Folk and Land, 1975). This environment would be the surface of a stable supratidal sabkha.

THEORETICAL STRATAFORM MODELS FOR THE ORIGIN OF THE KENNECOTT ORE BODIES

Renfro (1974) proposed a sabkha model for strataform copper and other metalliferous ore bodies that is based on the fact that coastal sabkhas and their related evaporite facies prograde seaward across adjacent algal-mat facies. Upon burial the algal-mat facies become saturated with hydrogen sulfide generated by anaerobic bacteria. Concurrently, the trailing, landward edges of coastal sabkhas are buried by prograding terrigenous clastics of the desert. As sabkhas migrate basinward, terrestrial-formation water eventually must pass upward through the buried, strongly reducing algal mat in order to reach the surface of evaporation.

Terrestrial formation water initially contains low pH and high Eh and thus can mobilize and transport trace amounts of such elements as copper, silver, lead, and zinc. Renfro's model moves metal to the site of deposition through the agency of oxygenated terrestrial ground water that migrates seaward through the transgressed substrata under the sabkha flat and upward to a surface of evaporation. The metals are precipitated on contact with hydrogen sulfide-laden algal mats.

A model using Renfro's concepts to the formation of the Kennecott ore bodies requires an exposed terrane of Nikolai Greenstone with its high disseminated copper content that is subjected to subaerial weathering. Meteoric waters weather the Nikolai Greenstone, and remove by solution the Cu^{++} ions. These ions are in solution and during the wet season are carried by streams to the prograding Chitistone sabkha sediments. When these meteoric waters reach the algal mat the Cu metals are reduced and precipitated interstitially as sulfides between the carbonate and anhydrite-gypsum mineral of the sabkhas. Later diagenetic and connate waters concentrate the copper sulfides into the massive ore bodies associated with the sabkha zebra beds.

Jackson and Beales (1967) gave a sedimentary basin evolution origin for the Mississippi Valley type lead-zinc low temperature 70-160°C stratabound ore bodies. During the normal evolution of a sedimentary basin the chemistry of escaping compaction-generated fluid will evolve through time. Gas and oil pools are associated with early diaganetic processes and metallic mineralization with later diagenetic processes. The principles which govern the localization of many ore bodies are sedimentary principles. Lead-zinc deposits of Mississippi Valley type are concentrated in sedimentary carbonate rocks because hydrogen sulfide forms and accumulates in carbonate reservoirs, and it subsequently acts as a precipitant of metallic sulphides. Ore bodies are found where regional permeable porous trends, acting as a "plumbing system" for escaping basinal saline connate waters that carry the ore metals, traverse local H_2S-bearing carbonate reservoirs.

Macqueen (1976) showed that the processes of hydrocarbon maturation and migration, second stage clay mineral dewatering, and Mississippi Valley-type mineralization all occur in the range of about 60° to 150°C.

Jackson and Beales (1967), Beales and Jackson (1967, 1968), Billings et al. (1969), Jackson and Folinsbee (1969), and Macqueen (1976) in their studies of the Pine Point deposits on the south shores of the Great Slave Lakes, Northwest Territories, Canada, found that the ore bodies form an integral part of the upper Pine

Point and Presqu'ile Formations. These elongate lens-shaped bodies range from a few hundred thousand to 10 million tons. Margins are sharp; most of the ore was deposited in open cavities and vugs. Colloform and crystalline sphalerite and galena are the only ore minerals; abundant marcasite, pyrite, calcite, and dolomite comprise the gangue. Evaporites, deposited in a supratidal (sabkha) environment, appear to have played a major role in the development of porosity that governed later dolomitization and ore emplacement. Beales and Jackson (1968, fig. 1:4) show that the mine walls of Presqu'ile dolomite have vuggy porosity developed by the solution of evaporites from the dolomite. The resulting vuggy porosity formed the main conduits for the ore-bearing fluids. Their Pine Point vugs are lined with conspicuous white dolomite rhombs. Billings, Kesler, and Jackson (1969), Bush (1970), Macqueen, Williams, Barefoot, and Foscolos (1975), and Macqueen (1976) pointed out that the Pine Point and other stratabound deposits in the Canadian Rocky Mountain belt show stratigraphic control and that the sources for the bulk of metals are the host rock themselves or more or less laterally equivalent basin facies, consisting of metalliferous sedimentary shales.

The Pine Point sedimentary ore genesis model shows many strong parallels with the Kennecott ore deposits in the Chitistone Limestone. The one major difference is that the Pine Point deposit consists of sphalerite-galena ore whereas the Kennecott deposit consists of copper ore. Possibly this difference exists because of the high copper content of the Nikolai Greenstone. The weathering and erosion of Nikolai Greenstone highlands during the Triassic and Jurassic could have produced copper-rich clays that were deposited in the basin adjacent to the sabkha deposits. A very clear parallel between Kennecott and Pine Point is the porosity caused by solution of the evaporite minerals. Beales and Jackson (1968, p. 5) stated "Several generations of dolomite are indicated probably beginning during barrier [reef] growth stages when widespread evaporitic pans formed and nodular coalescing growth of gypsum or anhydrite took place within the sediments. Later dolomite [limpid dolomite]...lines the cavities left when this gypsum dissolved and even later stage white vein dolomite and coarse calcite are probably associated with the stratafugic solution processes."

Their illustration ((Beales and Jackson, 1968, p. 4, fig. 1:4) of the host rock shows it to be similar in appearance to the zebra beds of the Chitistone in the Mother Lode mine; lithologically both host rocks consist of a fine dolomite matrix with vugs left by the dissolution of anhydrite-gypsum that were later lined with limpid dolomite and then filled with sparry calcite.

Fritz and Jackson's (1972) petrographic studies of dolomites from the Middle Devonian carbonate formations in the vicinity of the Pine Point lead-zinc deposits distinguished three dolomite generations: (1) supratidal (penecontemporaneous), (2) diagenetic (secondary), and (3) hydrothermal dolomites. The ore zones appear to be localized by a combination of initial depositional trends, subsequent tectonic features and a karst system. Hydrothermal development of the coarsely crystalline nature of the Presqu'ile dolomite is associated, at least in part, with emplacement of the ore as indicated by both field relationship and isotope studies.

Using the Jackson and Beales (1967), Beales and Jackson (1968), and Taylor, Macqueen, and Thompson (1975) models, a postulated theory for the Kennecott ore bodies consists of the deposition of deep-water starved basin shales formed adjacent to a reef and sabkha facies on the shelf platform that formed the Chitistone Limestone. The postulated shale facies of the Chitistone Limestone is not known from outcrop studies. A sedimentary section of 1,200 to 3,600 meters of Jurassic and Cretaceous sediments was deposited over the basinal shale and a geothermal gradient must have formed. At temperatures of 60° to 150°C the postulated black shale facies would generate mature oils, natural gas and brines containing metals (Cu) stripped from clay minerals. Brines from the basin sediments, probably as chloride complexes, migrated with the hydrocarbon and metal ions to the carbonate reservoirs, i.e., zebra beds of lower 100-130 meters of Chitistone Limestone. Finally, sulfide precipitation occurred where metal-bearing (Cu) brines encounter sulfur (anhydrite-gypsum beds and/or hydrocarbons) in the carbonate reservoirs.

CONCLUSIONS AND INTERPRETATIONS

Potter et al.'s (1977) ongoing mineralogical studies, Silberman et al.'s (1977) research, and our investigation all show the Kennecott ore deposits were characterized by a very complex history. Our interpretation of this history is illustrated in the following outline.

(1) Late Triassic to Middle Jurassic development of local small deposits best explained by the sabkha model.

(A) The ore bodies in the Jumbo, Bonanza, and Mother Lode mines are generally associated with the intertidal to supratidal zebra beds. The main inclined shafts at the Mother Lode and Bonanza mines were driven parallel to and just below the zebra beds. Bateman and McLaughlin (1920, p. 25, fig. 6) recognized this relationship in the Jumbo and Bonanza mines. Their "flat fault" which marks the base of the major ore bodies is approximately at the base of the zebra beds and 103 m (340 feet) stratigraphically above the Nikolai Greenstone.

(B) Study of the zebra bed within the mines and from outcrop samples indicates beds of early diagenetic dolomite and anhydrite formed in a supratidal sabkha environment. The interbedded dolomitic peloid, pisooid, and laminated caliches indicate these sediments were exposed to vadose weathering in hot semiarid conditions under the influence of fluctuating saline brines and rain water, that is, schizohaline environments. These conditions dissolved out the anhydrite and formed the clear dolomite vug linings.

(C) A marine transgression flooded the caliche-covered sabkha surface and deposited the overlying, relatively impervious pelecypod-echinoderm wackestones and packstones so that by the end of Triassic time there existed 800-1,000 m of sediments above the vuggy and highly porous sabkha-caliche. The sabkha and caliche formed a thin permeable porous horizon, which acted as a regional conduit for ore-forming fluids. In Late Triassic to Late Jurassic time the postulated black shale basinal facies could have generated hydrocarbonate and metalliferous copper brines that could have migrated upward into the porous zebra beds. This would have resulted in the formation of copper sulfide deposits.

(2) Development of favorable structural sites during the Late Jurassic-Early Cretaceous regional orogeny. Regionally the orogeny was accompanied by large-scale granitic intrusions, although none are known near the Kennecott mines. It is postulated that hydrothermal solutions generated during this orogeny derived copper from the Nikolai. The copper-laden solutions penetrated permeable parts of the Chitistone, specifically the porous sabkha bed where they acquired sulfur. The solutions partly replaced the primitive ore (Renfro model) and deposited copper sulfide-rich

lodes at favorable structural sites. Silberman et al.'s (1977) isotope studies on oxygen and carbon from the Chitistone Limestone and Kennecott ore are compatible with a sabkha mode of origin for the Kennecott deposits. This accounts for the shape of the ore bodies and is in accordance with Silberman et al.'s (1976) mineralogic and fluid inclusion studies.

ACKNOWLEDGMENTS

The underground studies in the Bonanza, Jumbo, and Mother Lode mines were conducted in 1974 in conjunction with M. L. Silberman of the U.S. Geological Survey, P. R. Holdsworth, former manager, Alaskan Exploration Inexco Mining Company, and Prof. Clay Smith and George Linn, New Mexico Institute of Mining and Technology. Dr. R. M. Lloyd, of Shell Development Company, helped Armstrong in examining the critical Donoho Peak section 74A-4. Outcrop and underground studies we made on the Kennecott mines in 1977 were done with the generous support of W. D. McCullough and C. B. Douthitt of Coastal Mining Company. We wish to express our appreciation for the generous help, critical review, and suggestions given by Robert N. Ginsburg, Eugene A. Shinn, Robert K. Park, Charles A. Repenning, J. W. Baxter, and George de Vries Klein. We wish to thank David L. Jones of the U.S. Geological Survey for the use of his excellent outcrop photographs.

REFERENCES CITED

Armstrong, A. K., and MacKevett, E. M., Jr., 1976, Relations between Triassic carbonate sabkhas and Kennecott-type copper deposits: _in_ Cobb, E. H., ed., The United States Geological Survey in Alaska: Accomplishments during 1975: U.S. Geol. Survey Circ. 733, p. 50-51.

Armstrong, A. K., MacKevett, E. M., Jr., and Silberling, N. J., 1969, The Chitistone and Nizina Limestone of part of the southern Wrangell Mountains, Alaska--A preliminary report stressing carbonate petrography and depositional environment: U.S. Geol. Survey Prof. Paper 650-D, p. D49-D62.

Bateman, A. M., and McLaughlin, D. H., 1920, Geology of the ore deposits of Kennecott: Econ. Geology, v. 15, p. 1-800.

Bathurst, R. G. C., 1959, The cavernous structure of some Mississippian _Stromatactis_ reefs in Lancashire, England: Jour. Geology, v. 67, p. 365-376.

_____1971, Carbonate sediments and their diagenesis: Amsterdam, Elsevier Publ. Co., 620 p.

Beales, F. W., and Jackson, S. A., 1967, Precipitation of lead-zinc ores in carbonate reservoirs as illustrated by Pine Point ore field, Canada: Inst. Mining and Metallurgy Trans., Sec. B, Applied earth science, v. 76, p. B278-B285.

_____1968, Pine Point--A stratigraphical Approach: Canadian Inst. Mining and Metall. Bull., v. 7, p. 1-12.

Billings, G. K., Kesler, S. E., and Jackson, S. A., 1969, Relations of zinc-rich formation waters, northern Alberta, to the Pine Point ore deposit: Econ. Geology, v. 64, p. 385-391.

Bush, P. R., 1970, Chloride-rich brines from sabkha sediments and their possible role in ore formation: Inst. Mining and Metallurgy Trans., v. 79, p. B137-144.

Dunham, R. J., 1962, Classification of carbonate rocks according to depositional texture: <u>in</u> Ham, W. E., ed., Classification of carbonate rocks: Am. Assoc. Petroleum Geologists Mem. 1, p. 108-121.

Dupont, E., 1881, Sur l'origine des calcaires devoniens de la Belgique: Acad. Royale Belgique Bull. Cl. Sci., ser. 3, v. 2, p. 264-280.

Esteban, Mateo, 1976, Vadose pisolites and caliche: Am. Assoc. Petroleum Geologists Bull., v. 60, p. 2048-2057.

Evamy, B. D., 1963, The application of a chemical staining technique to a study of dedolomitization: Sedimentology, v. 2, p. 164-170.

_____1967, Dedolomitization and the development of rhombohedral pores in limestone: Jour. Sed. Petrology, v. 37, p. 1204-1215.

_____1973, The precipitation of aragonite and its alteration to calcite on the Trucial Coast of the Persian Gulf: <u>in</u> Purser, B. H., ed., The Persian Gulf: Berlin, Springer-Verlag, p. 329-392.

Evans, G., Kinsman, D. J. J., and Shearman, D. J., 1964, A reconnaissance survey of the environment of recent carbonate sedimentation along the Trucial Coast, Persian Gulf: in Van Stratten, L. M. J. U., ed., Deltaic and shallow marine deposits: Amsterdam, Elsevier Publ. Co., p. 129-135.

Evans, G., Schmidt, V., Bush, P. R., and Nelson, H., 1969, Stratigraphic and geologic history of the sabkha, Abu Dhabi: Sedimentology, v. 12, p. 145-159.

Folk, R. L., 1965, Some aspects of recrystallization in ancient limestones: in Pray, L. C., and Murray, R. C., eds., Dolomitization and limestone diagenesis, a symposium: Soc. Econ. Paleontologists and Mineralogists Spec. Pub. 13, p. 14-45.

_____ 1974, The natural history of crystalline calcite carbonate: effect of magnesian content and salinity: Jour. Sed. Petrology, v. 44, p. 40-533.

Folk, R. L., and Land, L. S., 1975, Mg/Ca ratio and salinity: Two controls over crystallization of dolomite: Am. Assoc. Petroleum Geologists Bull., v. 59, p. 60-68.

Folk, R. L., Roberts, H. H., and Moore, C. H., 1973, Black phytokarst from Hell, Cayman Islands, British West Indies: Geol. Soc. America Bull., v. 84, p. 2351-2360.

Folk, R. L., and Siedlecka, A., 1974, The "Schizohaline" environment: Its sedimentary and diagenetic fabrics as exemplified by late Paleozoic rocks of Bear Island, Svalbard: Sedimentary Geology, v. 11, p. 1-15.

Friedman, G. M., 1959, Identification of carbonate minerals by staining methods: Jour. Sed. Petrology, v. 29, p. 87-97.

Fritz, P., and Jackson, S. A., 1972, Geochemical and isotopic characteristics of Middle Devonian dolomite from Pine Point, northern Canada: Internat. Geol. Cong., 24th, sec. 6, p. 230-243.

Fuller, J. G. G. M., and Porter, J. W., 1969, Evaporite formation with petroleum reservoirs in Devonian and Mississippian of Alberta, Saskatchewan, and North Dakota: Am. Assoc. Petroleum Geologists Bull., v. 53, p. 909-926.

Hillhouse, J. W., in press, Paleomagnetism of the Triassic Nikolai Greenstone, McCarthy quadrangle, Alaska: Canadian Jour. Earth Sciences.

Jackson, S. A., and Beales, F. W., 1967, An aspect of sedimentary basin evolution: The concentration of Mississippian valley-type ores during late stages of diagenesis: Canadian Petroleum Geology Bull., v. 15, p. 383-433.

Jackson, S. A., and Folinsbee, 1969, The Pine Point lead-zinc deposits, N.W.T., Canada, Introduction and paleoecology of the Presqu'ile Reef: Econ. Geology, v. 64, p. 711-741.

Kendall, C. G. S. C., and Skipwith, P. A. D., 1969, Holocene shallow-water carbonates and evaporites sediments of Khor al Bazam, Abu Dhabi, southwest Persian Gulf: Am. Assoc. Petroleum Geologists Bull., v. 53, p. 841-869.

Kendall, A. C., and Tucker, M. E., 1973, Radiaxial fibrous calcite: a replacement after acicular carbonates: Sedimentology, v. 30, p. 365-389.

Kinsman, D. J. J., 1966, Gypsum and anhydrite of recent age, Trucial Coast, Persian Gulf: _in_ Second symposium on salt, v. 1: Cleveland, Ohio, Northern Ohio Geol. Soc., p. 302-306.

_____1969, Modes of formation, sedimentary associations, and diagenetic features of shallow-water and supratidal evaporites: Am. Assoc. Petroleum Geologists Bull., v. 53, p. 830-840.

Kinsman, D. J. J., and Park, R. K., 1976, Algal belts and coastal sabkha evolution, Trucial Coast, Persian Gulf: Recent Model for interpreting stromatolite environments: Developments in Sedimentology, no. 20, Elsevier, p. 421-433.

Lecompte, M., 1937, Contribution a la connaissance des recifs du Devonian de l'Ardenne: sur la presence de structures conservees dans des efflorescences cristallines du type "_Stromatactis_": Belgique Mus. Royal Hist. Nat. Bull., v. 13, p. 1-14.

_____1954, Quelque donnes relatives a la genese et aux caracteres ecologiques des recifs du Frasnien de l'Ardenne: _in_ Brussels, Belgique Inst. Royal Sci. Nat., Victor Van Straelen, Directeur... 1925-1954, vol. Jubilaire I, p. 153-194. Transl. by P. F. Moore, 1959: Internat. Geology Rev., v. 1, no. 7, p. 1-23.

Lees, A., 1961, The Waulsortian reefs of Eire: A carbonate mudbank complex of lower Carboniferous age: Jour. Geology, v. 69, p. 101-109.

_____1964, The structure and origin of the Waulsortian (lower Carboniferous) "reef" of west-central Eire: Royal Soc. London Philos. Trans., ser. B., v. 247, p. 483-531.

Logan, B. W., Read, J. F., and Davies, G. R., 1970, History of carbonate sedimentation, Quaternary Epoch, Sharks Bay, Western Australia: in Carbonate sedimentation and environments, Shark Bay, Western Australia: Am. Assoc. Petroleum Geologists Mem. 13, p. 38-84.

MacKevett, E. M., Jr., 1965, Preliminary geologic map of the McCarthy C-6 quadrangle, Alaska: U.S. Geol. Survey Misc. Geol. Inv. Map I-494.

_____1970, Geologic map of the McCarthy C-5 quadrangle, Alaska: U.S. Geol. Survey Geol. Quad. Map GQ-899.

_____1974, Geologic map of the McCarthy B-5 quadrangle, Alaska: U.S. Geol. Survey Geol. Quad. Map GQ-1146.

_____1976, Gèologic map of the McCarthy quadrangle, Alaska: U.S. Geol. Survey Misc. Field Studies Map MF-773A, scale 1:250,000.

Macqueen, R. W., 1976, Sedimentary zinc and lead, Rocky Mountains belt, Canadian Cordillera: Geoscience Canada, v. 3, p. 71-81. igs.

Macqueen, R. W., Williams, G. K., Barefoot, R. R., and Foscolos, A. E., 1975, Devonian metalliferous shales, Pine Point region, District of Mackenzie: Canada Geol. Survey Paper 75-1, Part A, p. 553-556.

McKee, E. D., and Gutschick, R. C., 1969, History of Redwall Limestone of northern Arizona: Geol. Soc. America Mem. 114, p. 726.

Morlot, A. von, 1848, Sur l'origine de la dolomie (Extr. d'une lettre de M. A. de Morlot a M. Elie de Beaumont): Acad. Sci. Comptes Rendus, Paris, v. 26, p. 311-315.

Park, R. K., 1976, A note on the significance of lamination in stromatolites: Sedimentology, v. 23, p. 379-393.

Potter, R. W., II, Silberman, M. L., Nissenbaum, Arie, and Matthews, Alan, 1977, Mineralogy and isotope geochemistry of the Kennecott massive copper sulphide deposits, Alaska [abs.]: Geol. Assoc. Canada, Abs. with Prog. (in press).

Purser, B. H., and Evans, G., 1973, Regional sedimentation along the Trucial Coast, southeast Persian Gulf: _in_ Purser, B. H., ed., The Persian Gulf: Berlin, Springer-Verlag, p. 211-231.

Purser, B. H., and Loreau, J. P., 1973, Aragonitic supratidal encrustations on the Trucial Coast, Persian Gulf: _in_ Purser, B. H., ed., The Persian Gulf: Berlin, Springer-Verlag, p. 343-376.

Read, J. F., 1974, Calcrete deposits and Quaternary sediments, Edel Province, Shark Bay, Western Australia: in Evolution and diagenesis of Quaternary carbonate sequences, Shark Bay, Western Australia: Am. Assoc. Petroleum Geologists Mem. 22, p. 250-282.

Renfro, A. R., 1974, Genesis of evaporite-associated stratiform metalliferous deposits--A sabkha process: Econ. Geology, v. 69, p. 33-45.

Ross, R. J., Jr., Jaanusson, V., and Friedman, I., 1975, Lithology and origin of Middle Ordovician calcareous mud mound at Meiklejohn Peak, southern Nevada: U.S. Geol. Survey Prof. Paper 871, 48 p.

Scholle, P. A., and Kinsman, D. J. J., 1974, Aragonitic and high Mg calcite from the Persian Gulf--A modern analog for the Permian of Texas and New Mexico: Jour. Sed. Petrology, v. 44, p. 904-916.

Schwarzacher, W., 1961, Petrology and structure of some lower Carboniferous reefs in northwestern Ireland: Am. Assoc. Petroleum Geologists Bull., v. 45, p. 1481-1503.

Shearman, D. J., and Fuller, J. G., 1969, Anhydrite diagenesis, calcitization and organic laminites, Winnipegosis Formation, Middle Devonian, Saskatchewan: Bull. Canadium Petroleum Geology, v. 17, p. 496-525.

Shearman, D. J., Khouri, J., and Tara, S., 1961, On the replacement of dolomite by calcite in some Mesozoic limestones from the French Jura: Geol. Soc. London Proc., v. 72, p. 1-12.

Shinn, E, A., 1969, Submarine lithification of Holocene carbonates in the Persian Gulf: Sedimentology, v. 12, p. 109-144.

Shinn, E. A., Lloyd, R. M., and Ginsburg, R. N., 1969, Anatomy of a modern carbonate tidal-flat, Andros Island, Bahamas: Jour. Sed. Petrology, v. 39, p. 1202-1228.

Silberman, M. L., Matthews, A., Potter, R. W., II, and Nissenbaum, A., 1977 (in press), Stable isotope geochemistry and sulphide mineralogy and K/Ar age study of the Kennecott massive sulphide deposits, Alaska--continued: The United States Geological Survey in Alaska: Accomplishments during 1976: U.S. Geol. Survey Circ.

Silberman, M. L., Potter, R. W., II, and Nissenbaum, Arie, 1976, Stable isotope, sulphide mineralogy, fluid inclusion, and K-Ar age study of the massive sulphide deposits at Kennecott: in Cobb, E. H., ed., The United States Geological Survey in Alaska: Accomplishments during 1975: U.S. Geol. Survey Circ. 733, p. 51-52.

Taylor, G. C., Macqueen, R. W., and Thompson, R. I., 1975, Facies changes, breccias, and mineralization in Devonian rocks of Rocky Mountains, northeastern British Columbia: Canada Geol. Survey Paper 75-1, part A, p. 577-585.

Wilson, J. L., 1967, Carbonate-evaporite cycles in lower Duperow Formation of Williston basin: Bull. Canadian Petroleum Geology, v. 15, p. 230-312.

_____1970, Depositional facies across carbonate shelf margins: Gulf Coast Assoc. Geol. Soc. Trans., v. 20, p. 229-233.

_____1975, Carbonate facies in geologic history: Berlin, Springer-Verlag, 471 p.

Wood, G. V., and Wolfe, M. J., 1969, Sabkha cycles in the Arab/Darb Formation of the Trucial Coast of Arabia: Sedimentology, v. 12, p. 165-191.

Figure 1. Index map of Alaska showing the approximate area underlain by the Chitistone and Nizina Limestones and part of the McCarthy 1° by 3° quadrangle showing locations of Chitistone stratigraphic sections that were studied.

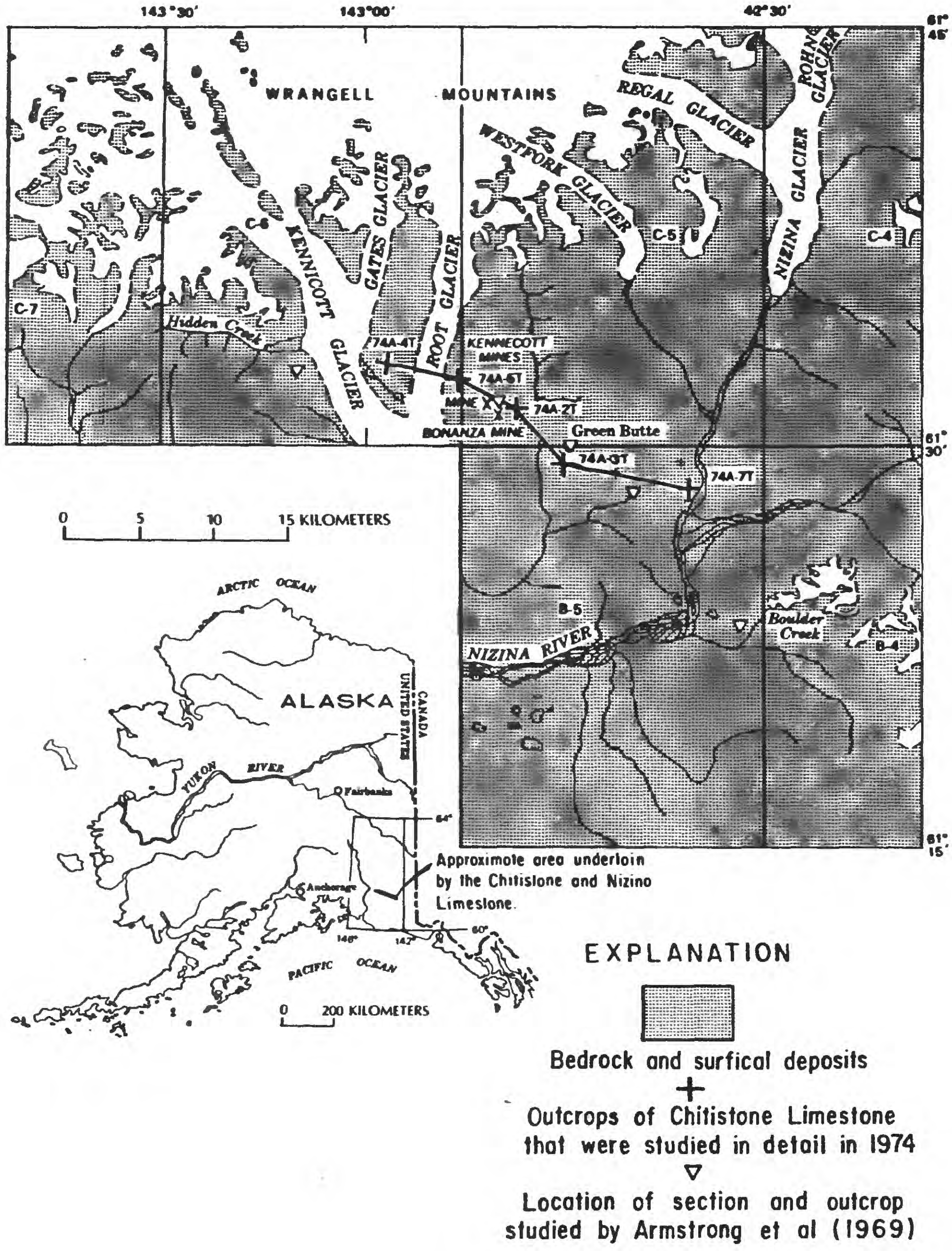

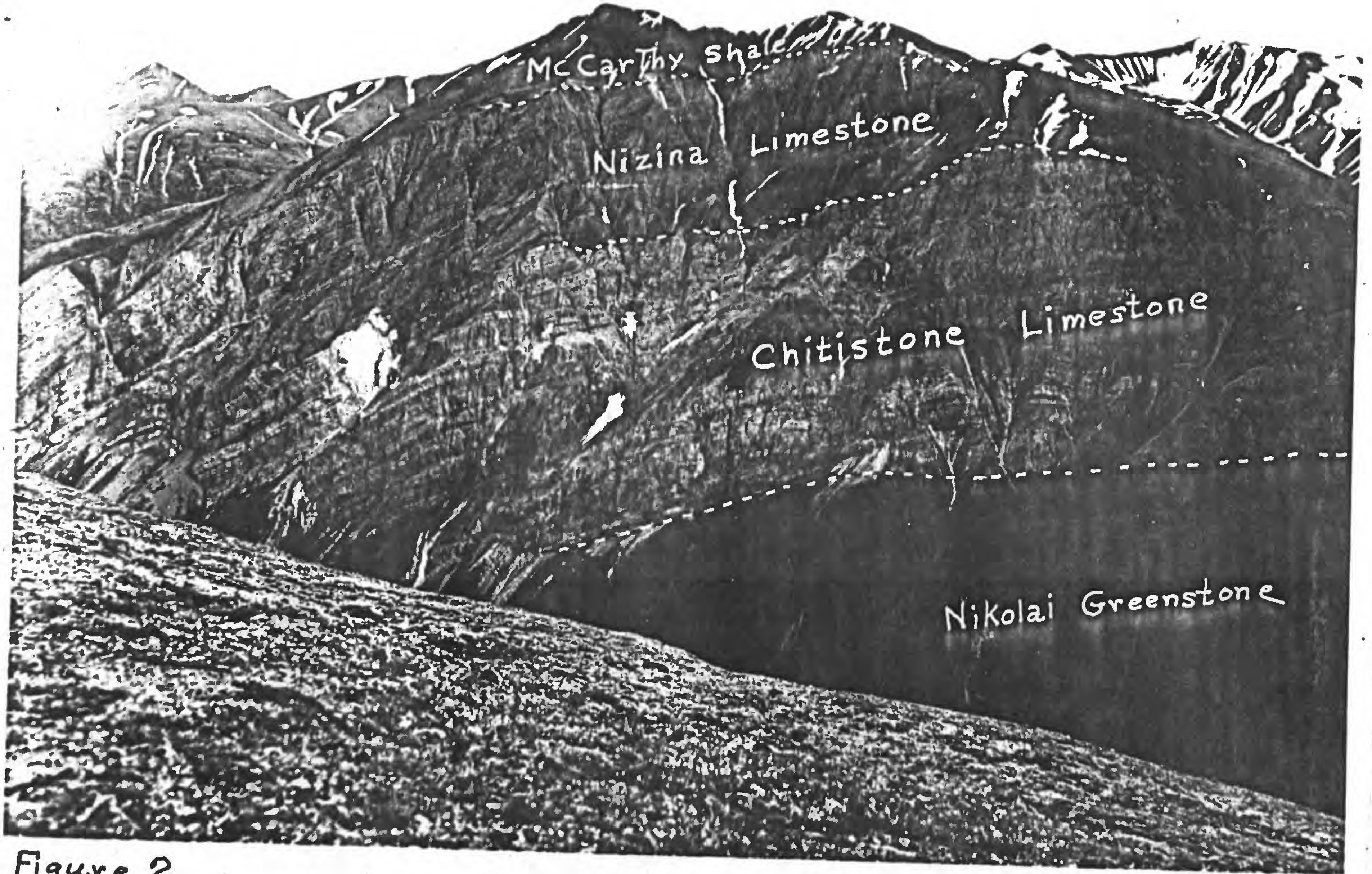

Figure 2

Figure 2. The west face of Green Butte as viewed from the hills west of McCarthy Creek. Relief on the west face is 1,082 m.

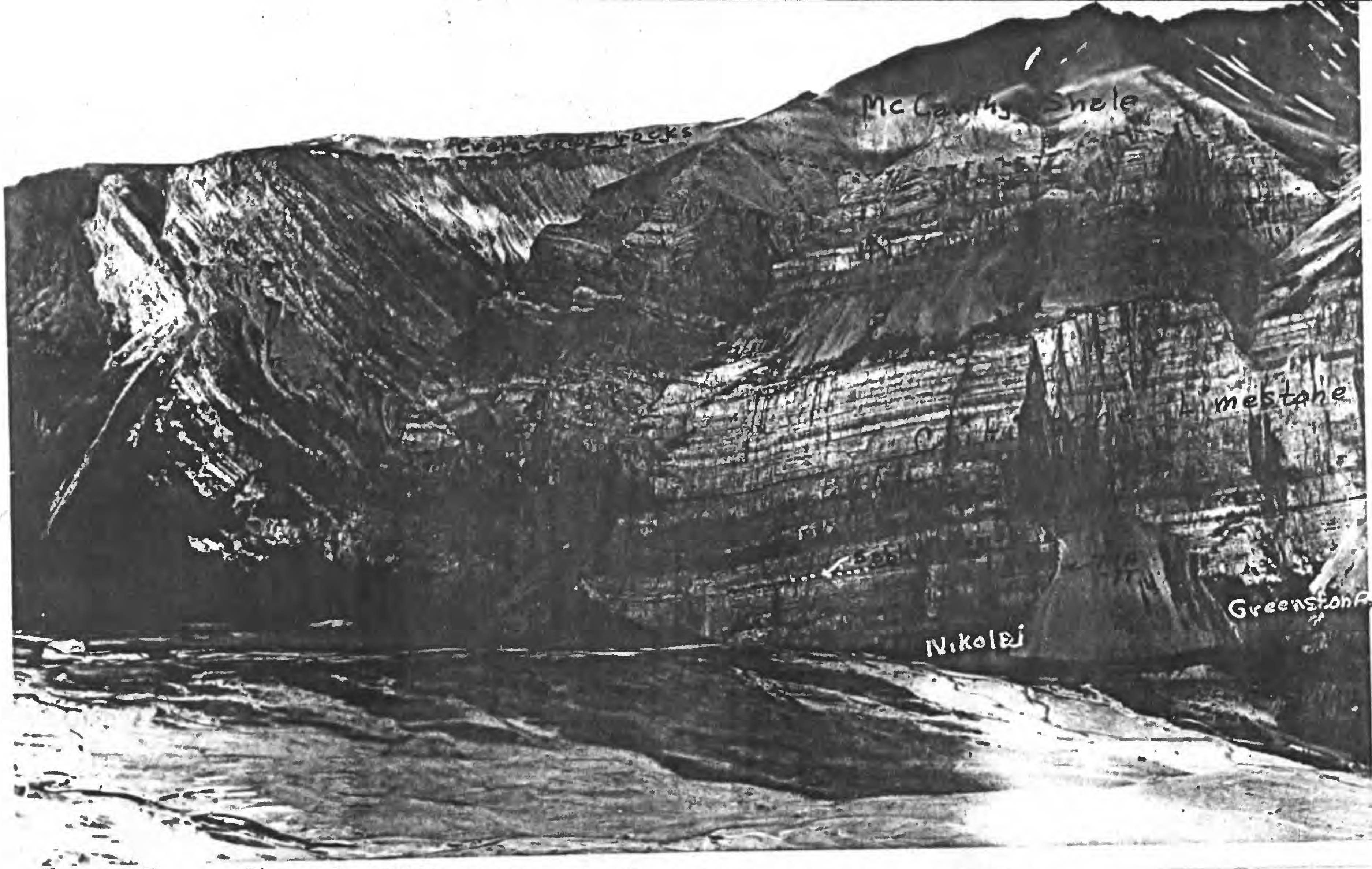

Figure 3

Figure 3. Cliffs on the west side of the Nizina Valley with relief approximately 1 km. The folded Triassic rocks are unconformably overlain by Albian and younger Cretaceous rocks. Location of the Nizina River study section 74A-7T is marked.

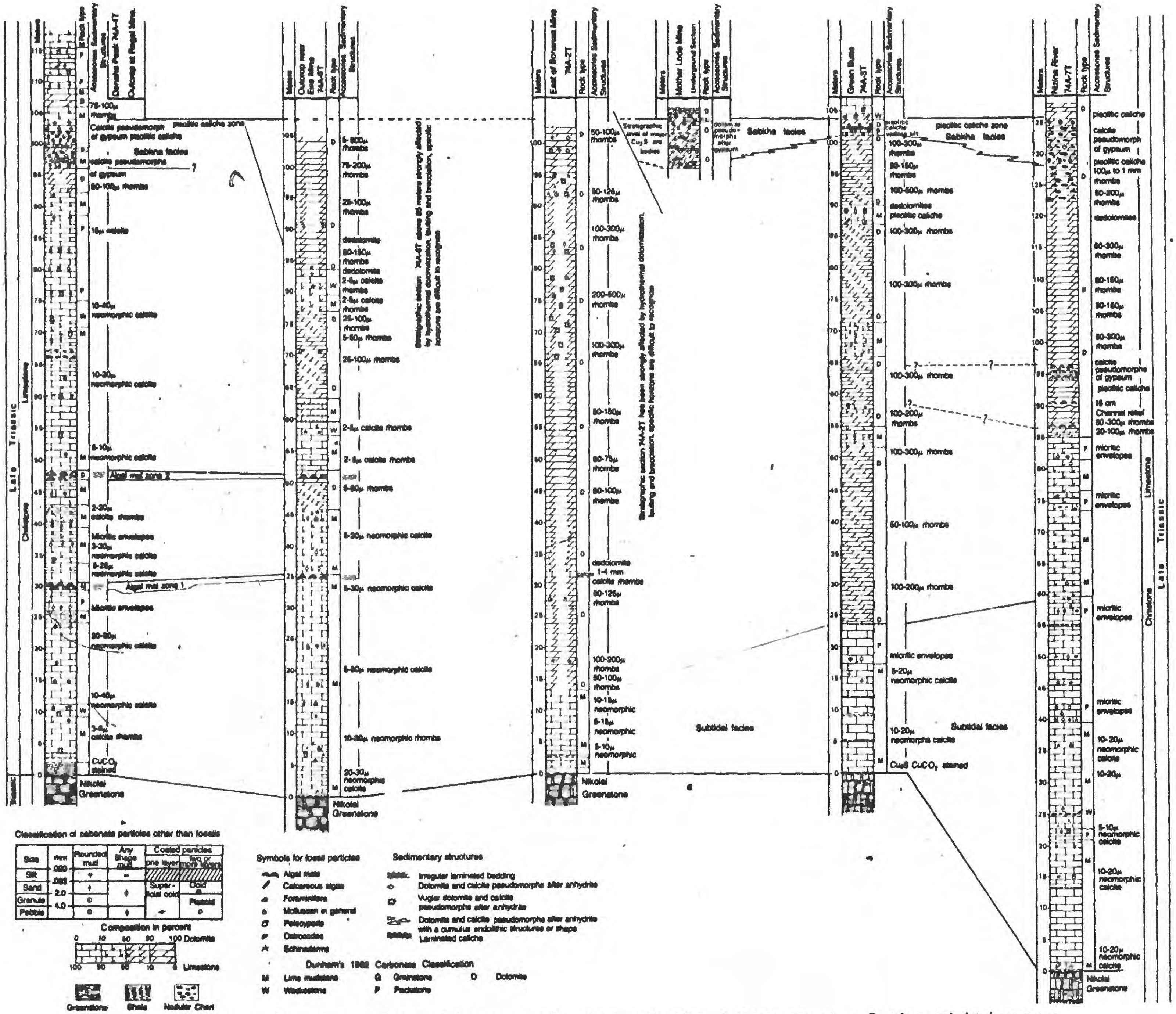

Figure 4. Stratigraphic correlation of the lower part of the Chitistone Limestone and the lithologies and sedimentary structures.

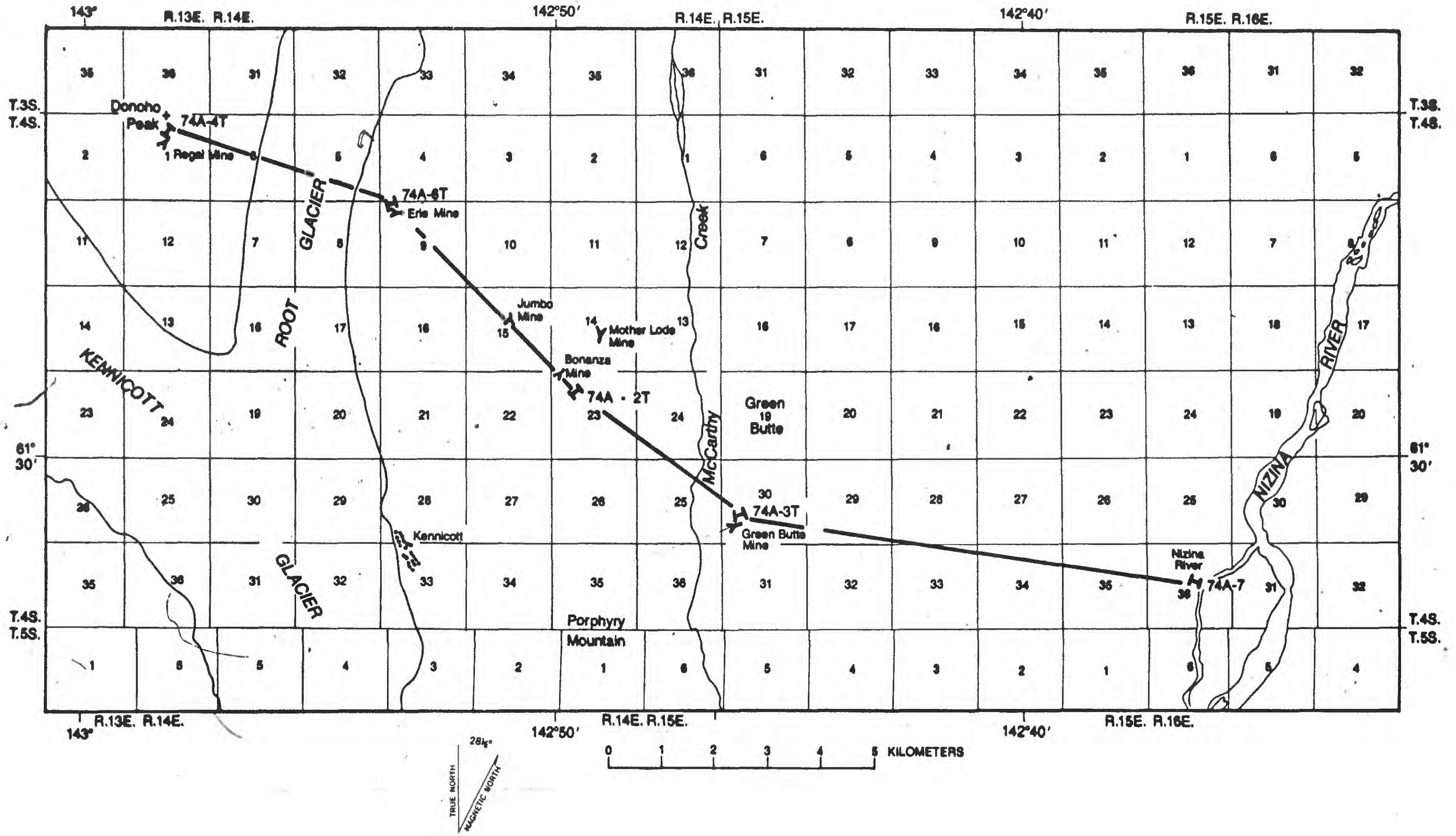

Figure 5. Index map showing location of measured stratigraphic sections.

Fig. 5

Figure 6

Specimens are from the Donoho Peak section, 74A-4T. The number in meters refers to the stratigraphic position above the base of the Chitistone Limestone.

Figure A. Lime mudstone aggrading neomorphism has produced calcite rhombs in the 10- to 20-um size. Shows faint outlines of peloids with smaller size calcite rhombs darker color. 15 meters.

B. Laminae, dolomitic-peloid lime mudstone, laminations are interpreted to be intertidal algal mats. 31 meters.

C. Peloid packstone to grainstone. The darker colored peloids appear to have a micritic envelope, and their surfaces covered with fibrous cement. Many peloids, as in the upper right corner of figure B contain in their center dolomite rhombs. The space between peloids is filled with sparry calcite. 37 meters.

D. Laminated dolomitic-peloid lime mudstone laminations are interpreted to be intertidal algal mats. 48 meters.

E. Dolomitic lime mudstone; in thin section the rock is peloid. The outline of part of a peloid can be seen in the lower right-hand side of the photomicrograph and is composed of smaller size calcite rhombs. The matrix between pellets contains a higher percentage of dolomite rhombs in the 10-20 um size and larger 5- to 20-um size calcite crystals. 69 meters.

Figure F. Peloid packstone. The peloids are clearly shown as lighter colored rounded areas to the left side of photograph. The peloid contains higher amounts of clay minerals between the calcite rhombs, and the matrix between peloids is formed by larger 5- to 12-um-size calcite rhombs. 88 meters.

TOP

Fig 6

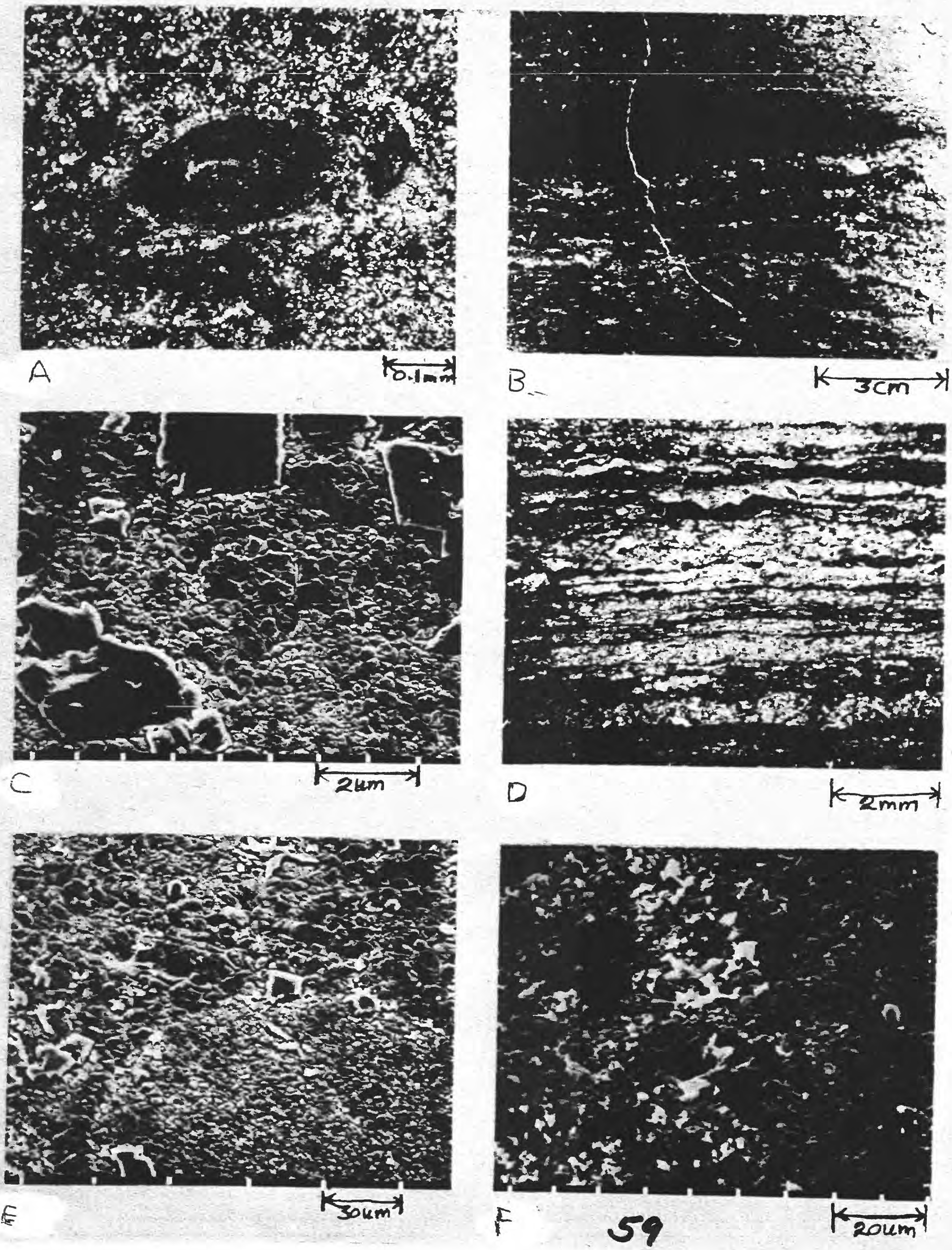

Figure 7

Specimen A is from the Donoho Peak section, 74A-4T. The numbers in meters refer to the stratigraphic position above the base of the Chitistone Limestone.

Figure A. Dolomitic-molluscan-echinoderm peloid packstone. Most molluscan fragments are now micritic envelopes, peloids contain dolomite rhombs; the calcite has undergone aggrading neomorphism. The peloids have radial fibrous calcite cement on their surface, space between peloids is sparry calcite. Arrow points to dolomite rhombs which have formed within the micrite of some peloids. 115 meters.

Specimens B-F are from the Nizina River section, 74A-7T. The numbers in meters refer to the stratigraphic position above the base of the Chitistone Limestone.

B, C. B, Brachiopod? shell fragment with possible geopedal filling in a matrix of micrite and pseudosparry calcite. C, SEM photomicrograph of limestone composed of 5- to 25-um-size calcite crystals, no apparent dolomite or clay minerals. This specimen in thin section (fig. B, above) is a peloid molluscan packstone which shows evidence of aggrading neomorphism. 42 meters.

D. Dolomitic limestone; dolomite is in clusters formed by 10- to 30-um-size subhedral rhombs, calcite matrix is 2 to 15 um in size. In thin section the rock is a peloid packstone with selective dolomitization of some of the peloids. 74 meters.

Figure 7--continued

Figures E, F. Dolomite and calcite. This specimen is from an outcrop bed 95 meters above the Nikolai Greenstone and has the same fabric as the zebra beds of the Mother Lode and Bonanza mine ore horizons. A polished surface of this rock is shown on Figure 20, C. The fine-grained dolomite matrix (DM) is shown on figure E; the large, zoned limpid dolomite (LD) is also marked; the final void filling by sparry calcite is shown by (CS). In figure F a thin fracture filled with calcite is seen on the left side of the photomicrograp This fracture with its sparry calcite filling cuts the dolomite matrix, the limpid dolomite rhombs, and the vug filling sparry calcite.

Fig 7 -

Top

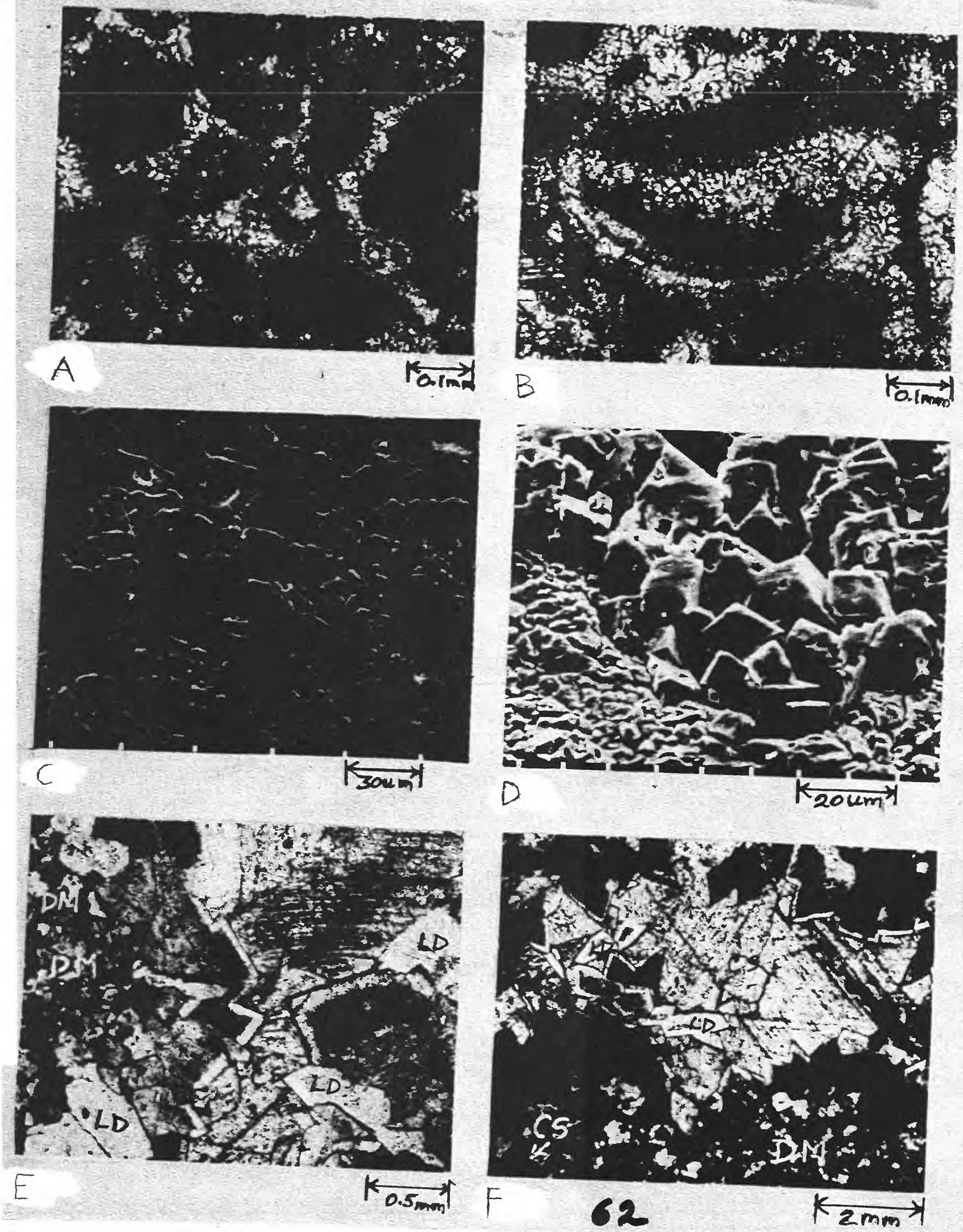

Figure 8

Specimens are from the Nizina River section, 74A-7T; 135 m. The numbers in meters refer to the stratigraphic position above the base of the Chitistone Limestone. Specimens A and B are SEM photomicrographs, specimen C is plane transmitted light photomicrographs.

Figures A. The large circular light-gray bodies are the etched surface of the pisooids, the large triangular-shaped gray area is sparry calcite (SC). The large rhomb shapes which stand out in relief are dolomite rhombs; the irregular light-gray area within the pisooid is also dolomite.

B. Enlargement of the bands within the pisooids reveals they are composed of alternating percentages of dolomite rhombs and calcite rhombs. The dolomite is shown by its sharp relief.

C. Pisooids, by transmitted light; many of the pisooids are covered by fibrous calcite. The large areas between pisooids are filled by sparry calcite.

Figure 8--continued

Specimens are from the Green Butte section, 74A-3T; 103 m. The numbers in meters refer to the stratigraphic position above the base of the Chitistone Limestone.

Figures D-F. Pisooid caliche, dolomitic limestone.

D, SEM view of a pisooid, showing small areas of calcite within the pisooid. The outer rims of some of the pisooids on the right side of the photomicrograph show rims of larger dolomite rhombs on the pisooids. Sparry calcite between rhombs is shown as dark-colored depressions between pisooids.

E, Large-scale SEM view of the small dolomite rhombs, that are 2 to 5 um in size which form the pisooids; upper left center of photomicrographs show larger, gray dolomite rhombs in the 10- to 30-um size; these dolomite rhombs are deposited on the exterior of the pisooids. Lower left half of photograph shows sparry calcite rhombs which contain small 1- to 2-um dolomite rhomb inclusions.

F, Pisooid caliche; dolomitic limestone thin section in plane light, composed of various-sized pellets, peloids, and pisooids, sparry calcite cement between particles.

Fig 8

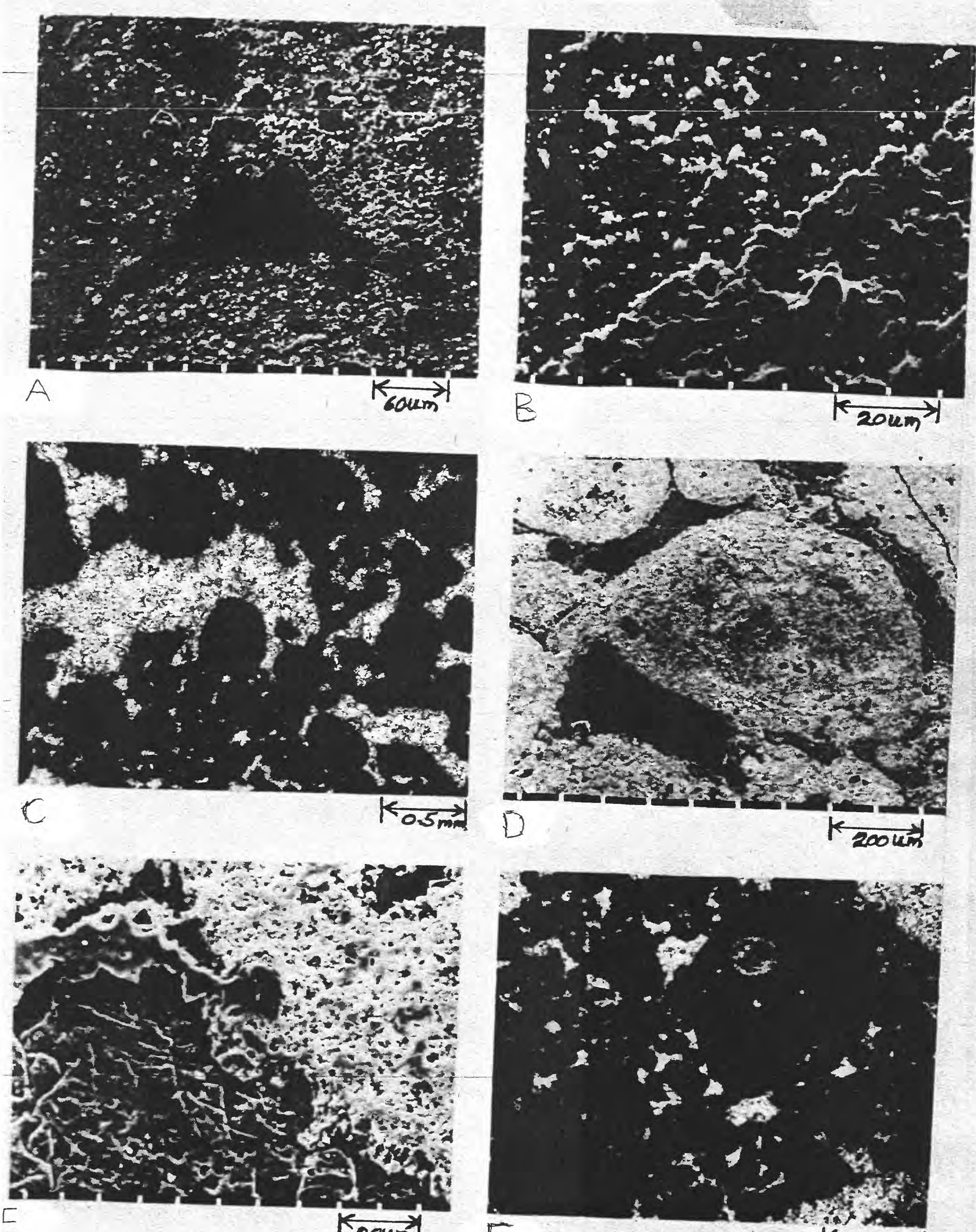

Figure 9. Detailed graphic illustration and interpretation of environment of deposition of the complex carbonate rock lithologies from 95 to 110 m in the Donoho Peak section 74A-4T. Note the laminated and pisooid caliches at 97 to 97.8 m and 99.7 to 100 m interbedded with supratidal carbonates.

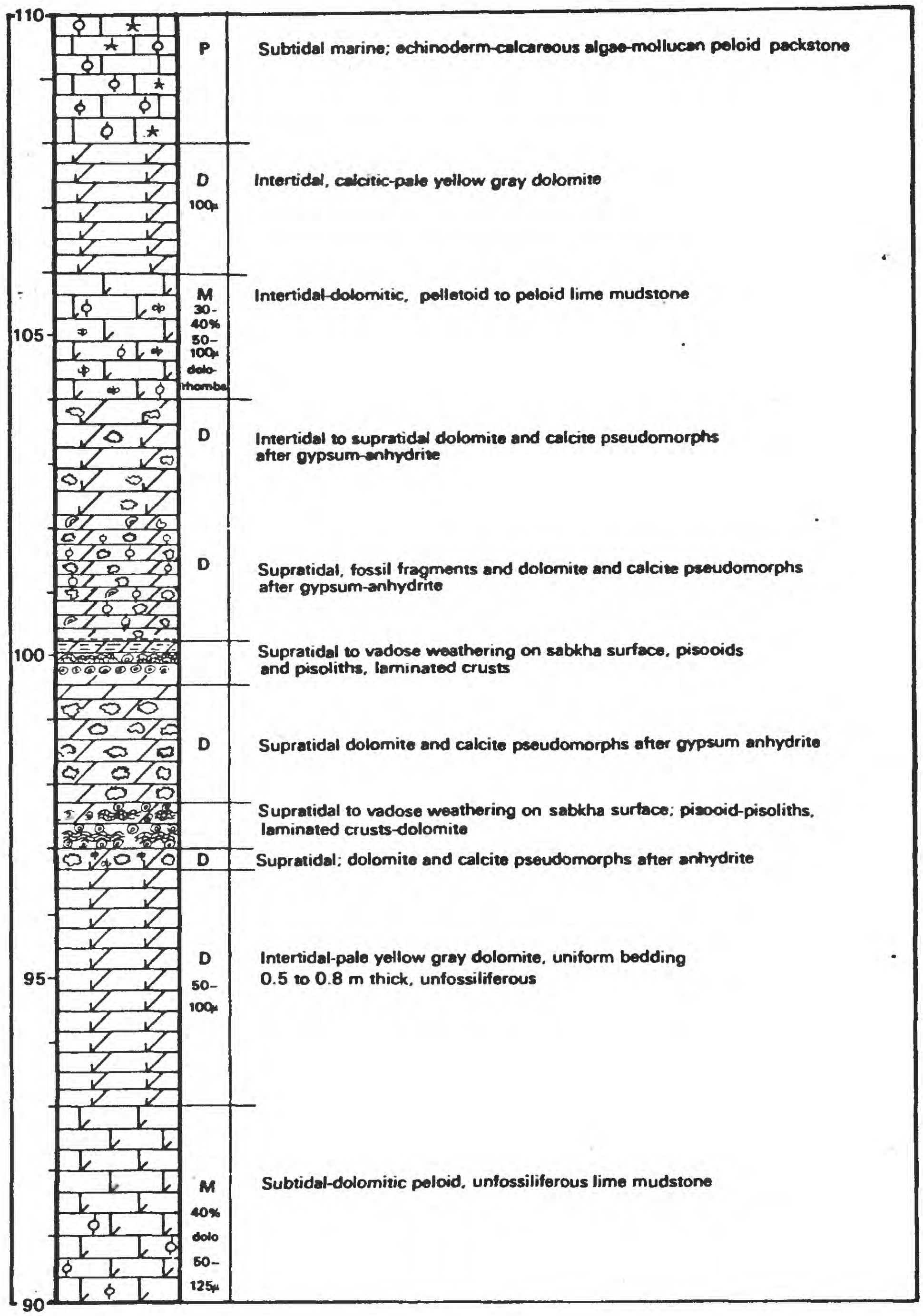

Fig 9

Figure 10

Specimens are from the Donoho Peak section, 74A-4T. The numbers in meters refer to the stratigraphic position above the base of the Chitistone Limestone.

Figure A. Dolomitic-lime mudstone, dark areas are dolomitic lime mudstones composed of very small crystals of dolomite and calcite. The large limpid dolomite rhombs (LD) line the void walls. The void is filled by sparry calcite (SC). 99.7 meters.

B. Peloid lime mudstone. The peloids are composed of a mixture of very small dolomite and calcite rhombs. The arrows point to the subhedral to anhedral limpid dolomite rhombs which line the voids. The remainder of the void is filled by sparry calcite. This thin section is from the caliche beds. 100.3 meters.

C. Laminated crust, showing in lower part vesicles formed by overlapping upward "bubbles" and parallel laminations. Above parallel lamination are nontectonic breccias formed of broken crusts. 100 meters.

D. Enlarged view of laminae of crust with convex vesicles filled with small subhedral rhombs of clear dolomite and calcite. 100 meters.

E. Enlarged view of broken crust showing calcite filling.

Fig 10

Top

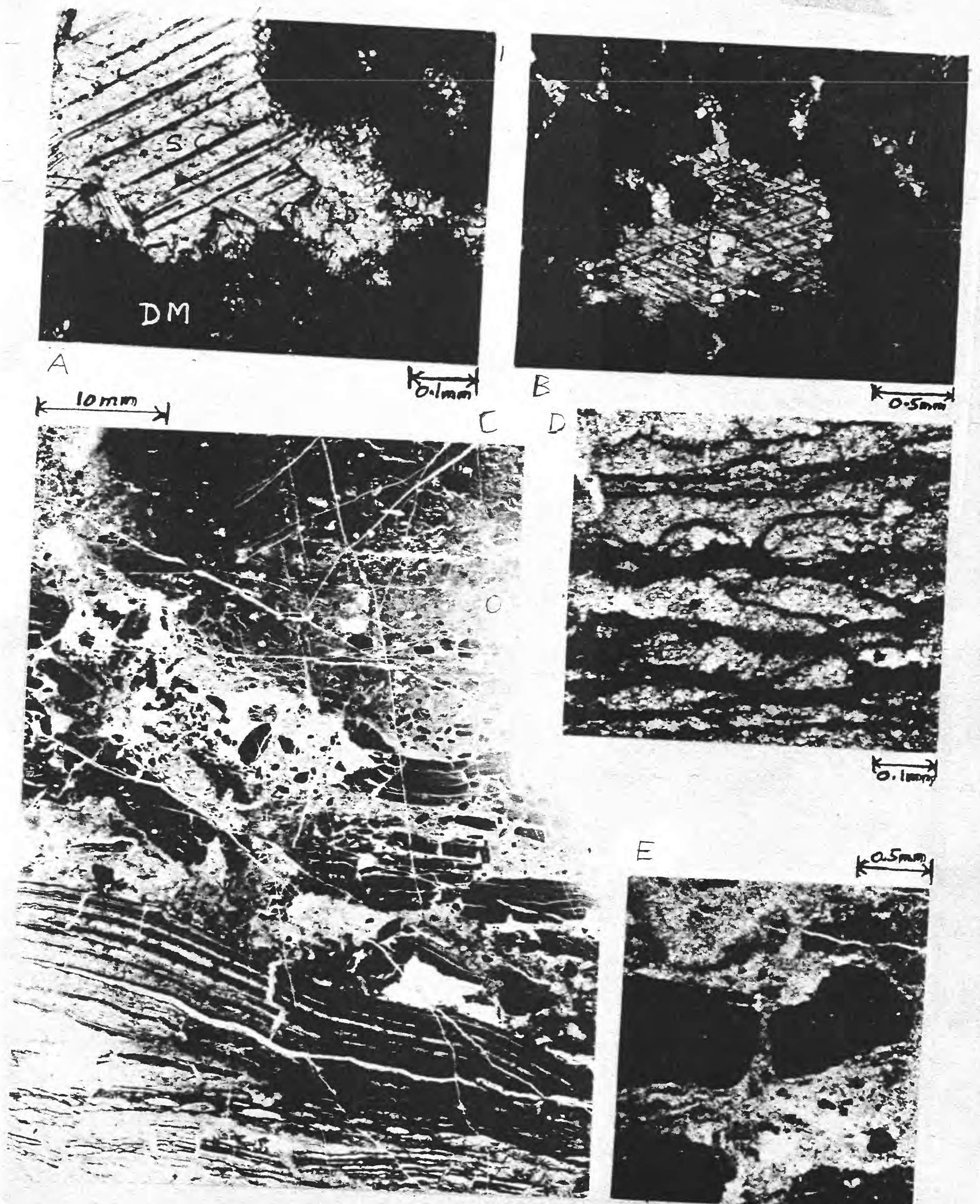

Figure 11

Specimens are from the Donoho Peak section, 74A-4T. The specimen was collected within and at 97.2 meters above the base of the Chitistone Limestone.

Figures A-D. Dolomitic-pisooid-caliche.

A, A view of textures illustrating packing and size range of pisooids, large clear areas are filled with rhombs of clear dolomite and sparry calcite. In lower part of photograph note reverse grading of pisooid.

B, Enlarged view of a pisooid showing banding and light and dark areas.

C, Pisooids and light-colored limpid dolomite (LD) void filling and final sparry calcite (SC) void filling in center of interareas.

D, Small pellets or pisooids beneath larger pisooid. Surface of pisooid is covered with small dolomite rhombs, center of voids are filled with calcite.

Fig. 11

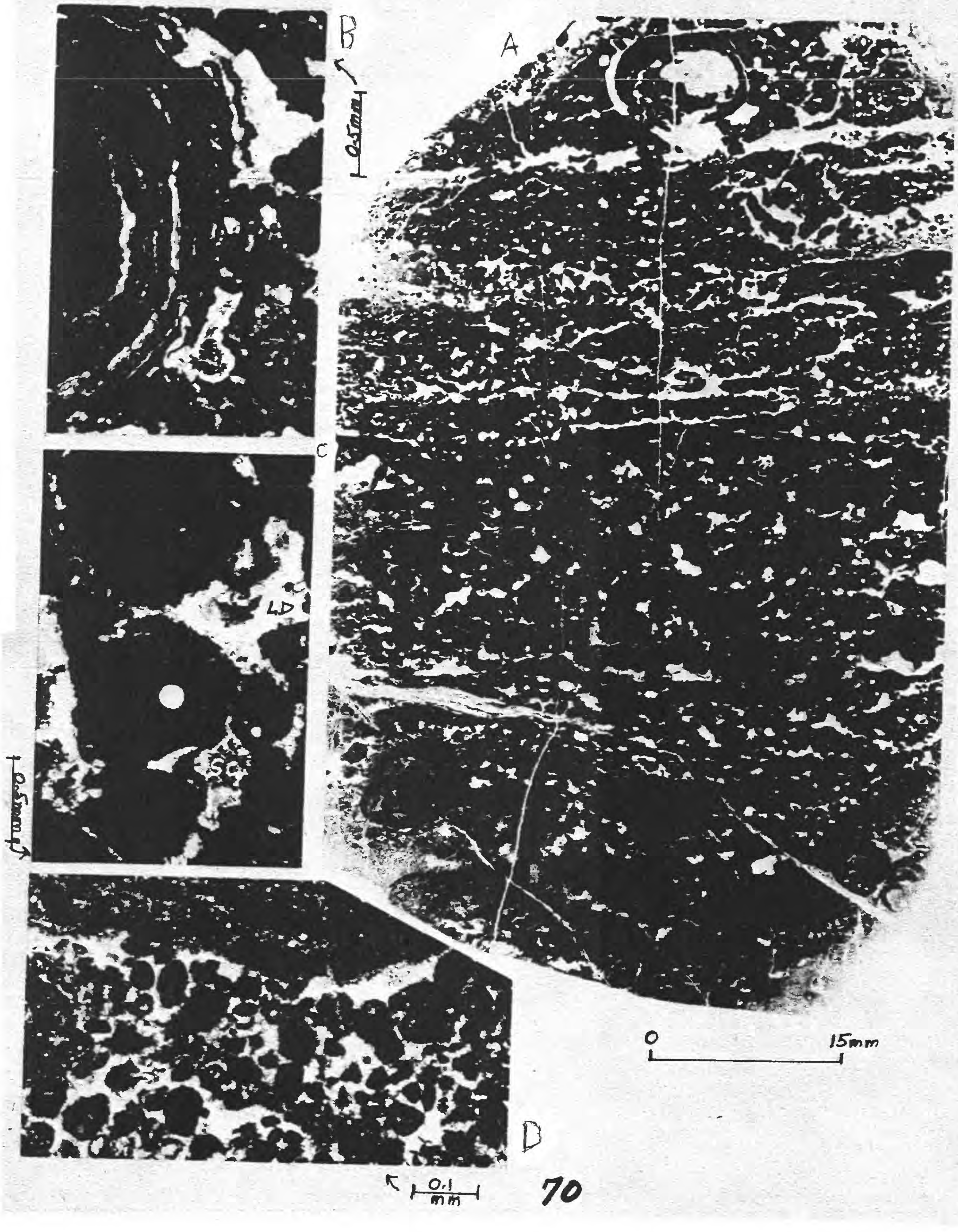

70

Figure 12

Specimen is from the Nizina River section, 74A-7T, from the Chitistone Limestone 130 meters above its base.

Figures A-D. Sedimentary breccia.

A, Photograph of a polished slab of the breccia. The dark dolomite matrix (DM) and birdseye-like structures and the nontectonic brecciation are clearly visible. The light-colored fibrous-like dolomite (DF) is clearly seen as is the overlying darker colored radiaxial fibrous calcite (CF). The white sparry calcite (SC) fills the center of the voids.

B, A transmitted light low magnification photograph of a thin section, which shows the fine-grained dolomite matrix (DM), the fibrous-like dolomite (DF), the radial fibrous calcite (CF), and the sparry calcite (SC).

C, Thin section of dolomite matrix (DM), thin band of fibrous-like dolomite (DF), quartz (Q), radial axial fibrous calcite (CF), and sparry calcite (SC), plane light.

D, Thin section (cross nichols), same symbols as above.

Fig. 12

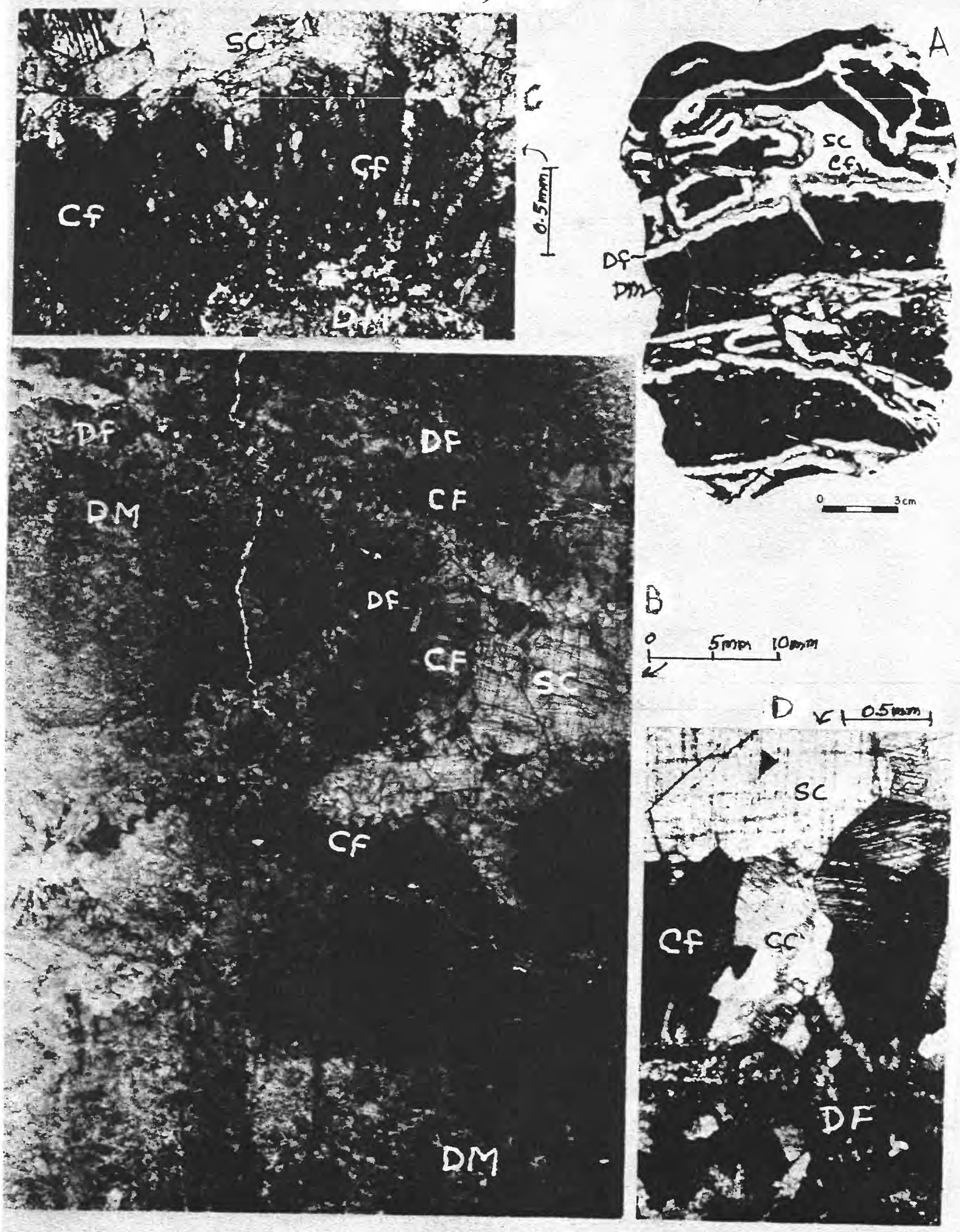

TOP
A
SC
CF
DF
DM
0
3cm
B
0
5mm
10mm
C
SC
CF
CF
0.5mm
D
DF
DF
DM
CF
DF
CF
SC
CF
DM
D
0.5mm
SC
CF
SC
DF

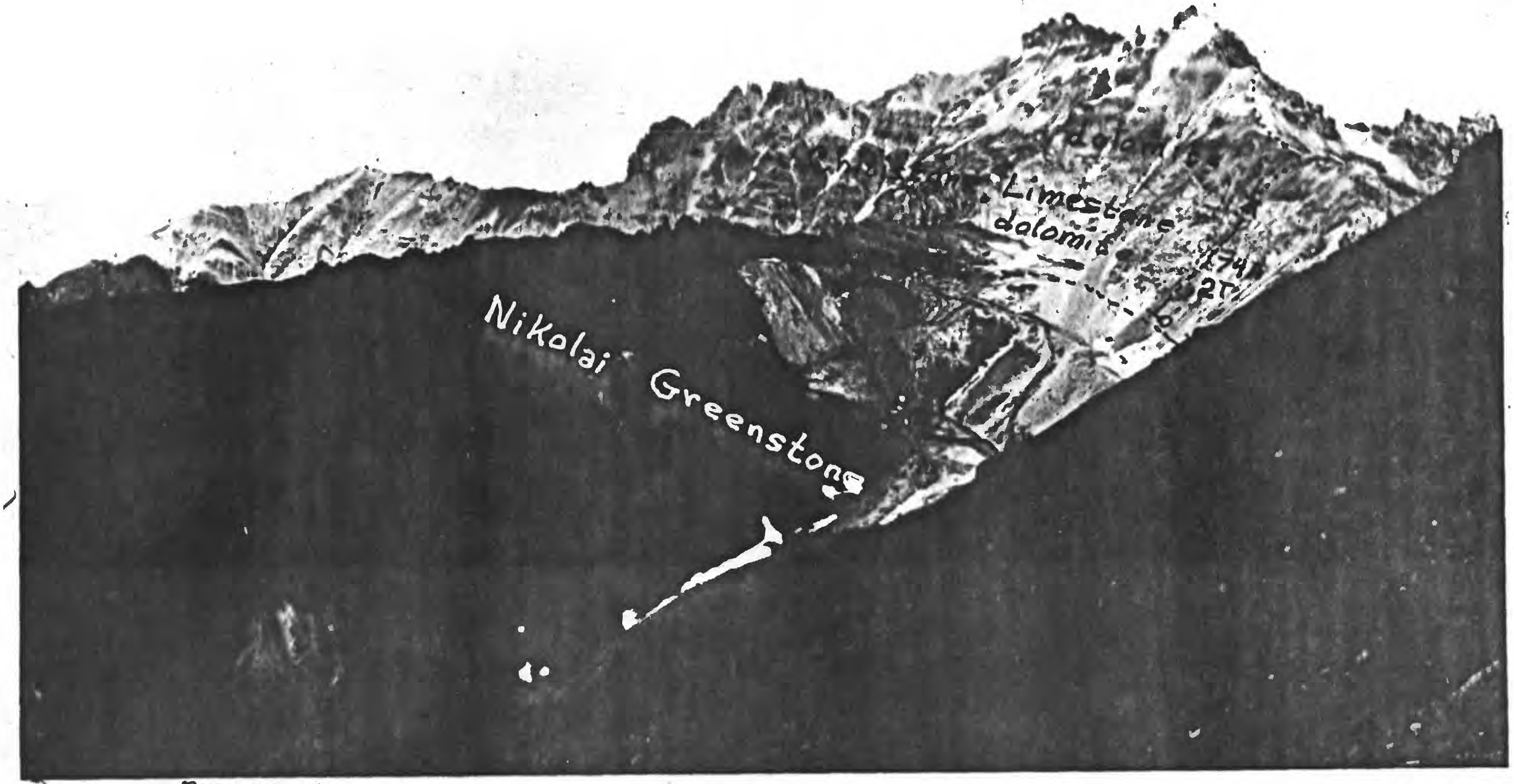

Figure 13
Figure 13

Figure 13. Photograph of Bonanza Ridge looking west toward the ruins of the Bonanza mine bunkhouse and power plant. The Glory Hole is on ridge above the power plant. The Chitistone on Bonanza Ridge is dolomitized and makes the irregular outcrop. Bedding planes are poorly preserved and the outcrop is vertically jointed.

Figure 14

Specimen shown in figure A is from the Bonanza Mine outcrop section, 74A-2T, and was collected at 4 meters above the Nikolai Greenstone-Chitistone Limestone contact.

Figure A. Argillaceous lime mudstone, calcite rhombs are between 5 to 20 um in size. The clay minerals are found between the calcite crystals. This argillaceous rock is typical of the lower 5 to 10 meters of the Chitistone found in the study area. EDAX X-ray analysis of the clays shows they are composed of Al, K, Ca, Si, Fe.

Specimens shown in figures B-F were collected in the Mother Lode mine at the 503-m (1,650-foot) level adjacent to the ore bodies (see figures 17 and 20). Specimens are from the zebra beds of the miners. Stratigraphic position of specimens is given in centimeters.

Figures B. Dolomite, with a cavity believed to be an anhydrite mold, lined by limpid dolomite (LD) and filled by sparry calcite (SC). Note fine fracture filled by sparry calcite (SCF), which cuts dolomite matrix (DM), limpid dolomite, and sparry calcite. 30 cm.

C. Dolomite; crossed nichols, typical anhydrite pseudomorph, dolomite matrix (DM), large crystals of limpid dolomite lining cavity (LD), sparry calcite center fill (SC), all cut by fracture filled with sparry calcite (SCF). See figure 19, E, for polished surface of this sample. 170 cm.

Figure 14--continued

Figures D. Dolomite; crossed nichols; typical zebra rock specimen (see figure 20, A, B, D), illustration represents filling of an anhydrite pseudomorph, dolomite matrix (DM), large crystals of limpid dolomite lining vug (LD), fracture filled with sparry calcite which crosscuts other minerals (CSF). 350 cm.

E, F. SEM photomicrographs. E, calcite filled vug, showing small dolomite rhomb inclusion within the calcite. Vug is lined by 200- to 300-um-size dolomite rhombs. F, fracture in dolomite filled by sparry calcite with inclusions of dolomite.

[redacted] FIG 14

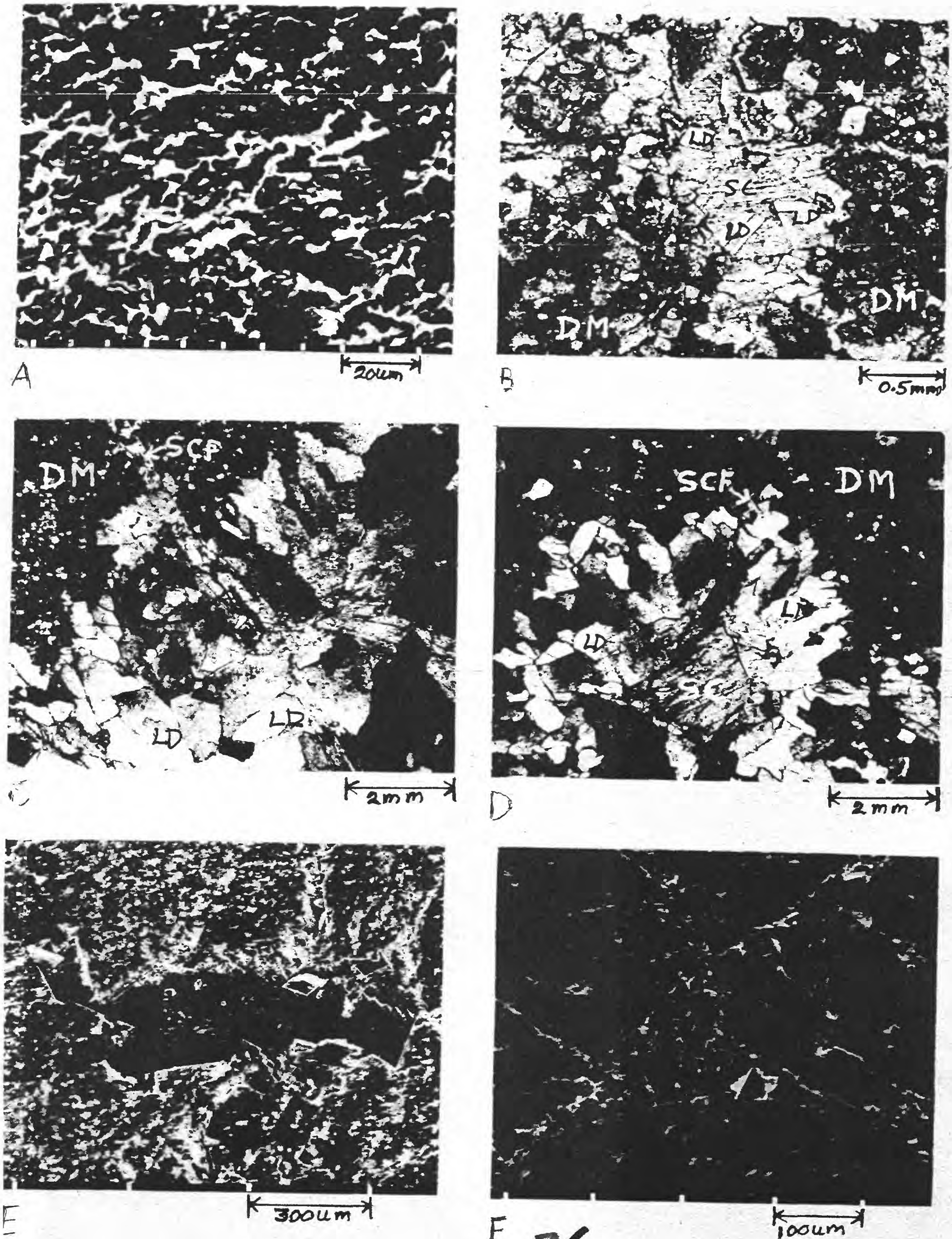

Diagrammatic cross section for Mesozoic carbonate facies

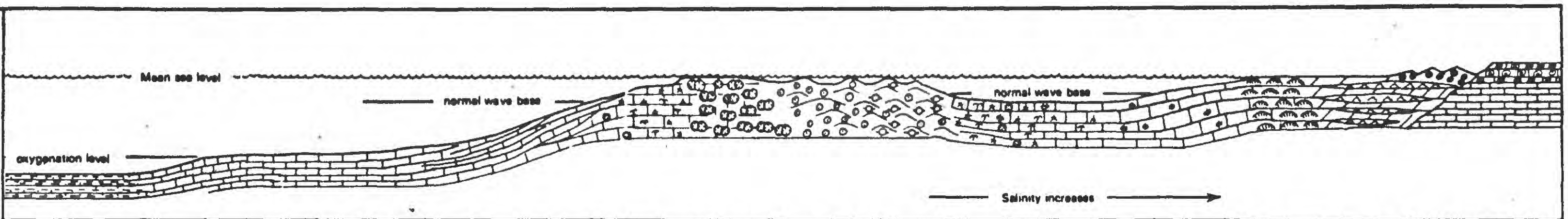

Facies and facies numbers	Basin-euxinic facies 1	Tidal Shelf facies 2	Toe-of-Slope carbonates 3	Foreslope 4	Organic reef Boundstone mass 5	Sands on edge of platform 6	Open platform 7	Restricted platform 8	Intertidal to supratidal facies 9	Vadose weathering of sabkha surface carbonate dune sands caliche-calcrete 10
Lithology	Shale, radiolarian cherts and siltstones.	Interbedded thin-to medium-bedded lime mudstone; dolomite and chert.	Interbedded limestone and dark gray shale.	Variable depending on water energy upslope. Sedimentary breccia and lime sand or lime mudstone.	Crust on accumulation of organic debris and lime mud. Massive limestone dolomite	Crinoid-bryozoan to ooid packstone and grainstone.	Variable. Carbonate bryozoan-crinoid packstone; chert common.	Finely and coarsely crystalline dolomite; dolomitic-crinoid bryozoan, wackestone and packstone dolomitic-pelletoid lime mudstone.	Irregularly laminated dolomitic lime mudstone and dolomite; anhydrite and calcite pseudomorphs of anhydrite common; algal mats.	Coated particles, peloid, pisolites, compound peloids, alternating microlaminae limpid dolomite rhombs.
Color	Dark brown to black	Gray to brown	Gray to dark brown	Gray to light gray	Light gray	Light gray	Light gray	Light gray to gray	Gray-yellow brownish red	Gray-light gray yellowish brown
Bedding and sedimentary structures	Very even millimeter laminations, rhythmic bedding, ripple cross laminations, burrows and worm trails on bedding surfaces.	Thoroughly burrowed. Thin to medium, wavy to nodular beds, bedding surfaces show diastems	Laminations may be minor, massive beds common, lenses of graded sediments; lithoclasts and exotic blocks	Slumps in soft sediments foreset bedding, exotic blocks	Massive to thick beds, some cross bedding- to massive organic structures or open framework with roofed cavities	Medium- to large scale cross bedding; festoons common.	Abundant burrows	Birdseye structures, algal mats on or near intertidal zone, stromatolites in very shallow water graded cross bedding.	Anhydrite-gypsum rhombs, bedded anhydrite, cracks chips, algal mats.	

Figure 15. Depositional model for the Upper Triassic carbonate facies of the Wrangell Mountains. Concepts for the model are from Wilson (1970, 1975).

Figure 16 Figure 15

Figure 16. Idealized and interpreted carbonate depositional cycles for the lower 130 m of the Chitistone Limestone. This model is based on the Donoho Peak outcrop section 74A-4T. Lithologic symbols are shown on figure 4.

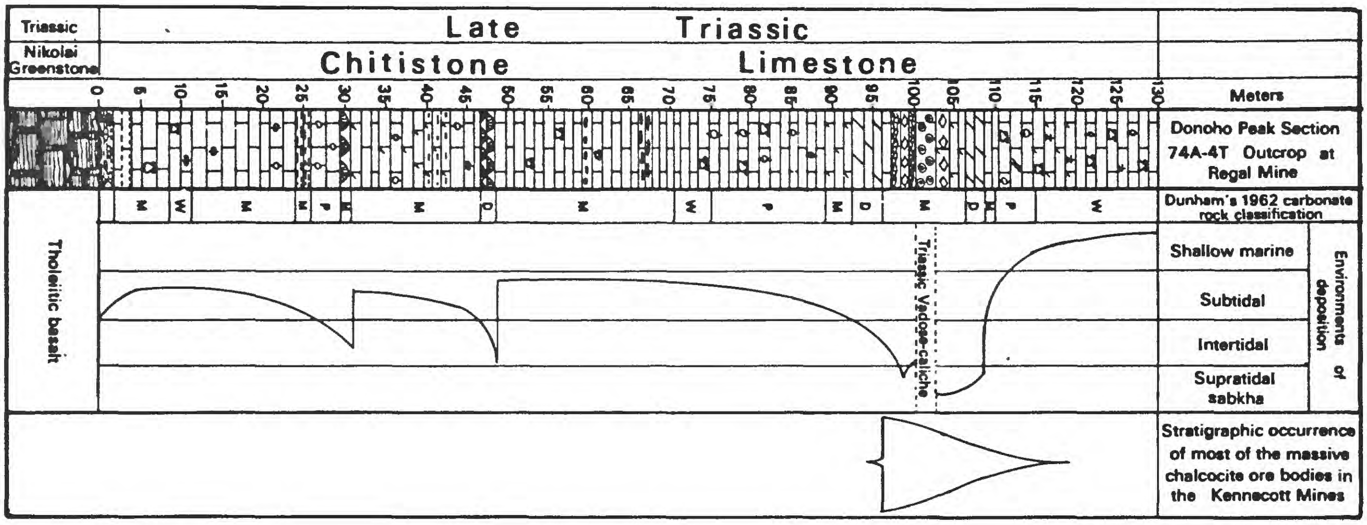

Figure 17. Probable sequence of alterations of a peloid-bioclastic grainstone as exemplified by a thin section from the Chitistone Limestone. A, Original sediments consisting of bioclasts of molluscans (Ab) with a micritic envelope, echinoderm, calcite bioclasts (cb), and peloids (P). B, First stage $CaCO_3$ cement. C, Dissolution of aragonite clasts. The micritic envelope and first stage $CaCO_3$ provides strength to molluscan bioclast molds. D, Complete cementation by second phase $CaCO_3$ cement, syntaxial overgrowth on crinoid calcite bioclasts. E, Many of the peloid sediments within the Chitistone Limestone show the development of dolomite (D) rhombs within the peloids and the development within the peloids of microspar (C) from the micrite. A peloid-molluscan echinoderm packstone would show a similar sequence of events. The micritic matrix may go to microspar, resulting in a rock which would be very similar in appearance to the above grainstone.

Fig 17

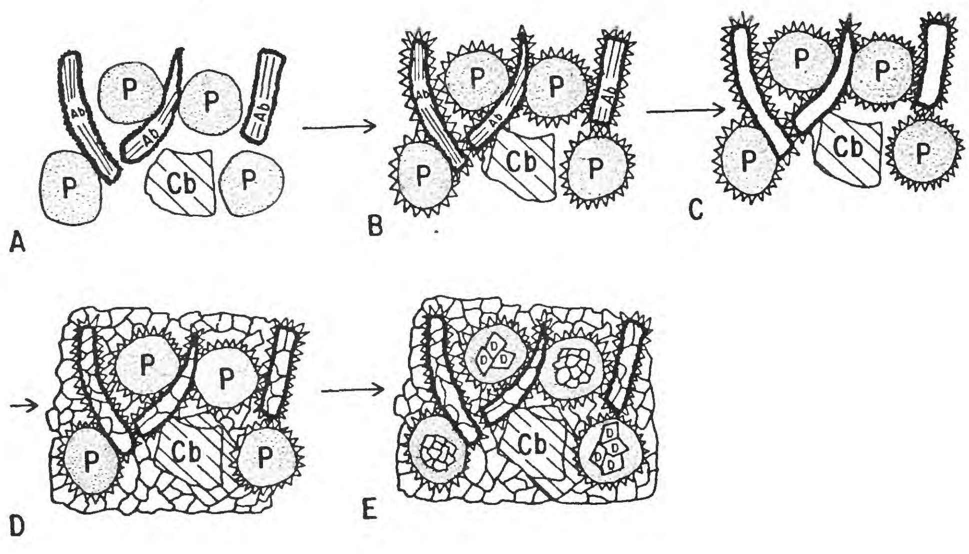

Figure 18. The 503-m (1,650-foot) level of the Mother Lode mine, of the wall rock, adjacent to the ore bodies. The beds dip about 30° to the right. The dark-colored area is the dolomite matrix rock, the light-colored areas are cavities lined with limpid dolomite and final void filling by sparry calcite. The beds which underlie the unit are uniform gray dolomite which have burrows and small-scale cut and fill structures. The beds which overlie these beds are coarse-grained dolomites with dolomite pseudomorphs of echinoderms. These structures resemble the Stromatactis of the literature. The white areas of the photograph are dolomite and calcite cavity fillings of what we interpret as pseudomorphs after interbedded anhydrite.

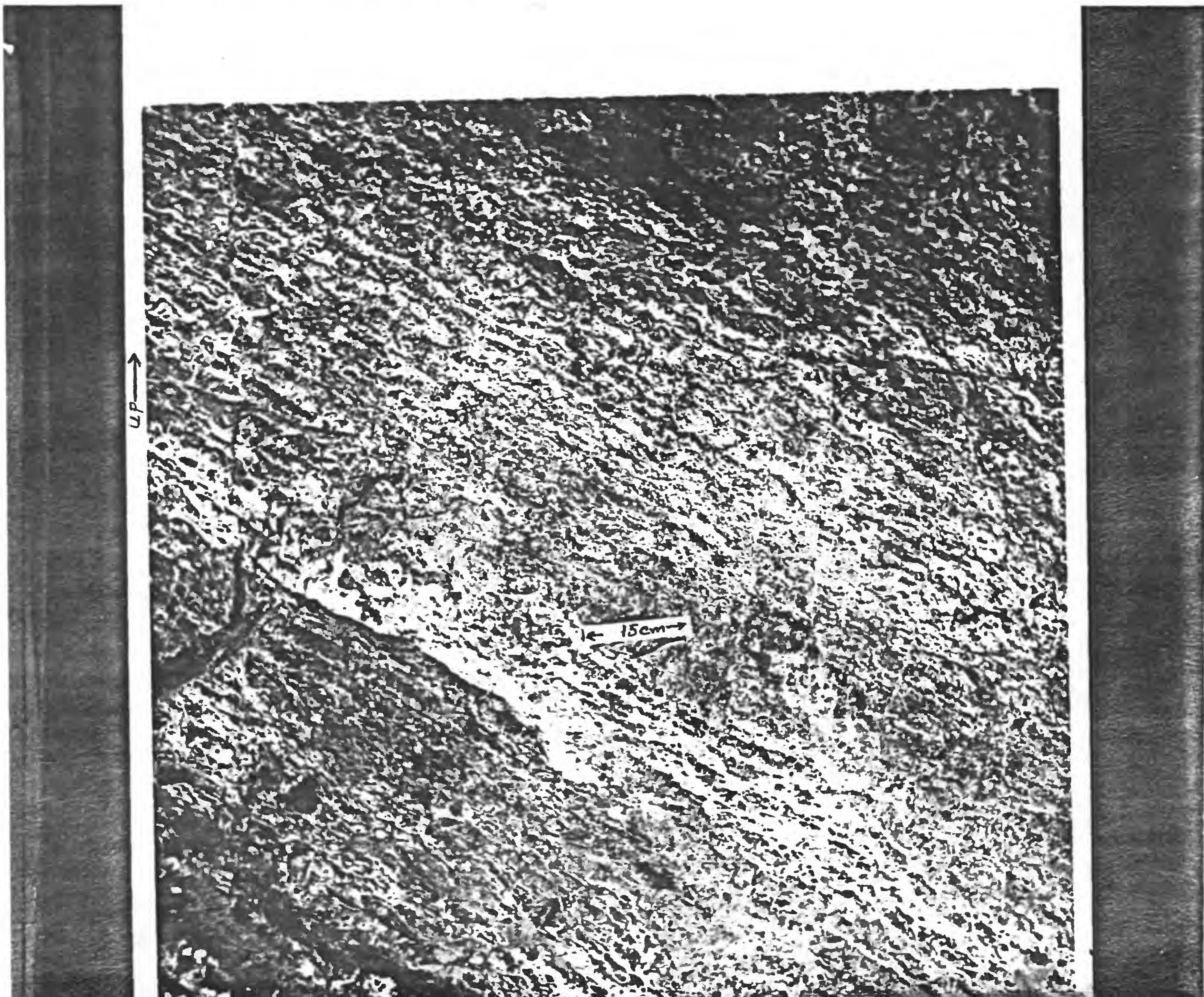

Figure 19

Specimens were collected in the Mother Lode mine at the 503-m (1,650-foot) level adjacent to the ore bodies (see figures 18, 21). Specimens are from the zebra beds of the miners. Stratigraphic position of specimen is given in centimeters.

Figures A, B. A, Photograph of polished surface of zebra rock, dark-colored areas are dolomite matrix, light-colored areas are limpid dolomite and calcite pseudomorphs of anhydrite.

B, Low magnification transmitted light photograph of a thin section. Fine-grained dolomite matrix (DM), anhydrite pseudomorphs, filled first by large limpid dolomite rhombs (LD), and final void filling by sparry calcite (SC); tectonic fracture, now filled by sparry calcite (SCF) crosscuts all textures. These fractures also contain copper mineralization. See figure 20, B, for SEM photomicrographs. 250 cm.

Figure 19--continued

Figures C, D. C, Photograph of polished surface of zebra rock; dark-colored areas are dolomite matrix, light-colored areas are limpid dolomite and calcite pseudomorphs of anhydrite.

D, Low magnification transmitted light photomicrograph of a thin section. Fine-grained dolomite matrix (DM), anhydrite pseudomorphs, filled first by large limpid dolomite rhombs (LD), and final void filling by sparry calcite (SC). Tectonic fracturing crosscuts all textures and the fractures are filled by sparry calcite (SCF) and copper minerals (CU). 200 cm.

E. Polished surface of zebra rock; dark areas are dolomite matrix, light-colored areas are limpid dolomite, and calcite pseudomorphs after anhydrite. See figure 14, C, for a thin section view of this rock. 170 m.

Fig. 19

Figure 20

All specimens are from the Chitistone Limestone.

Figures A. Photograph of a polished surface of the pisolitic and laminated crust found in the Chitistone Limestone, in the Donoho Peak outcrop section, 74A-4T, 97.2 meters above the Nikolai Greenstone-Chitistone Limestone contact. See figure 12, A-D for details of this specimen.

B. SEM photomicrograph of the dolomite matrix (DM) and a calcite-filled fracture (SCF) from the zebra bed at 250 cm in the Mother Lode mine (see figure 19, A, B, for details of rock specimen). Note the calcite filling (CSF) in the fracture contains some dolomite rhomb inclusions.

C. Photograph of a polished surface of a zebra bed texture from the Nizina River outcrop section, 74A-7T. The dark-colored areas are dolomite matrix, the light-colored areas are limpid dolomite and sparry calcite pseudomorphs after anhydrite. For details of this specimen see figure 7, E, F, for petrographic thin sections. Note that the polished surface of this specimen, in texture and petrography, is similar to a specimen collected from the Mother Lode mine zebra bed shown on figure 20, D and E, and on figure 19, B, C, E.

Figures D, E. Photographs of the polished surfaces of the specimens from the zebra beds of the Mother Lode mine at the 503-m (1,650-foot) level adjacent to the ore bodies (see figs. 18, 21). Figure D is from 350 cm and E is from 300 cm. A thin section photomicrograph of figure D is shown on this figure as F. The dark-colored areas are dolomite matrix and the light-colored areas are limpid dolomite and calcite pseudomorphs after anhydrite.

F. Low magnification photomicrograph of a thin section of a zebra bed specimen at 350 cm from the 503-m (1,650-foot) level of the Mother Lode mine. The thin section is made from the same sample as shown in figure D. This example of the zebra rock contains the dolomite matrix (DM), limpid dolomite (LP), and sparry calcite (SC) filling of the anhydrite pseudomorphs. The fractures which cut all of the above textures are filled with sparry calcite (CSF) and copper minerals (CU). See figure 14, E, F, for details of the dolomite and calcite pseudomorphs.

Fig. 20

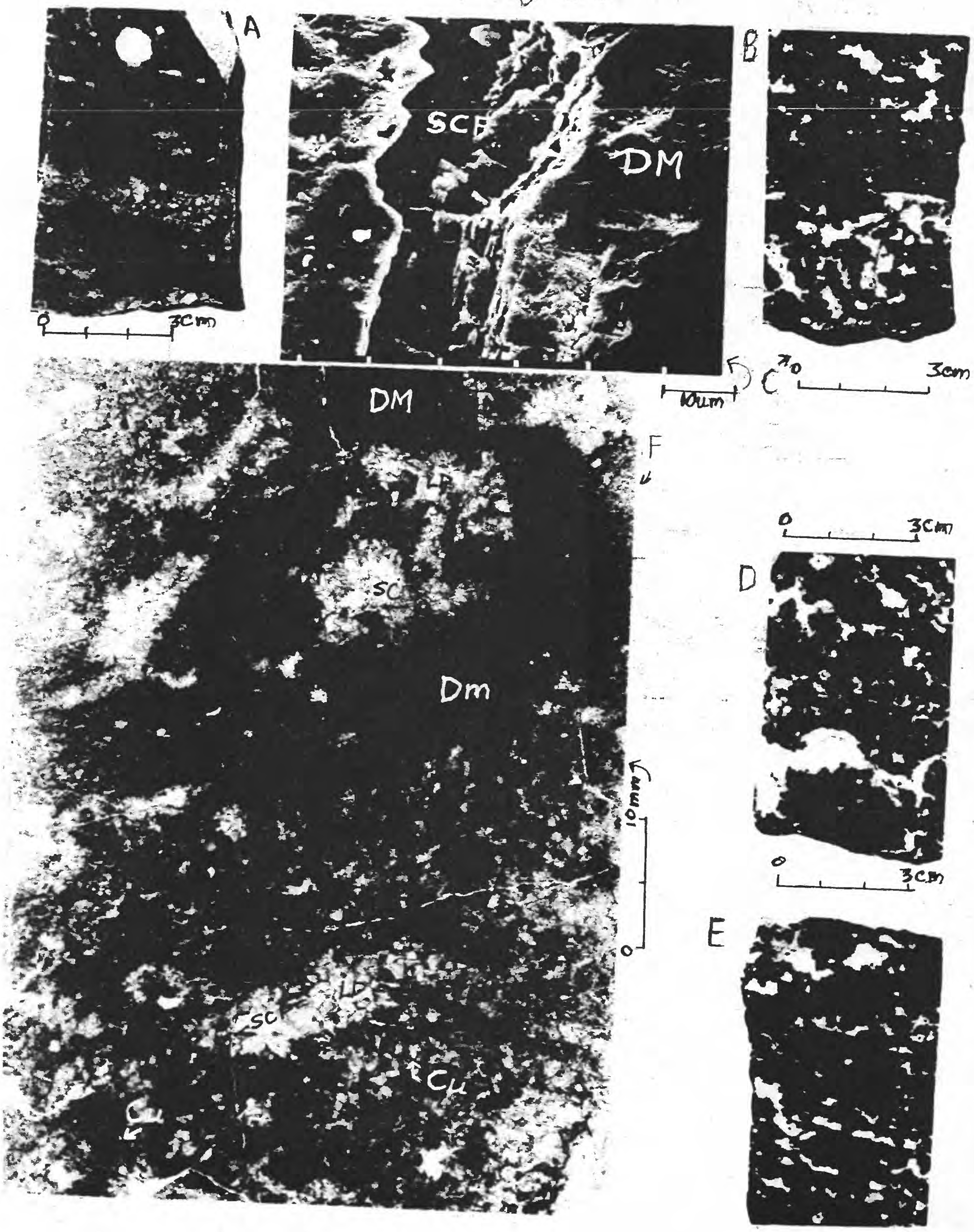

☆U. S. GPO: 1977-791-359

Figure 21. Illustration of the probable sequence of events in the development of the vug and cavity filling of the zebra bed. Concepts are from samples from the Mother Lode mine and the Nizina River section.